DÍAZ, REYNALDO THOMAS, Ph.D. High Resolution Visualization and Characterization of Cell Surface Adhesion Protein in Three-Dimensional Nanoscale Interphases. (2018)
Directed by Dr. Dennis LaJeunesse. 109 pp.

This dissertation studies microbial adhesion to surfaces using high magnification scanning particle beam microscopy. To study the interaction with the wings of cicada insects as our main surface of interest, the microbial model *Saccharomyces cerevisiae* with various levels of adhesive protein was used. Upon magnifying the cicada insect's wing one hundred thousand times, it evidences that the surface is composed of an even array of tiny nails. The past research as well as our group previous work have shown that the nanostructure surfaces like the cicada wing trigger responses in microbes that can range from cell proliferation to total cell-wall disruption. However, up to this day the reasons why certain nanostructured surfaces disrupt the cell-wall remained unclear. The central hypothesis of this thesis is to investigate the role of adhesion protein FLO11p found in S. cerevisiae cell wall and the surface topography at the nanoscale using scanning particle beam microscopy as the main technique.

A first step towards proving the central hypothesis was the development and use of immunogold labelling of FLO11p technique to be used with the scanning particle beam microscope and dispersive x-ray spectrometry. The image generated by secondary electrons and backscattered electrons has been traditionally used as correlative microscopy. However, incorporating electron energy dispersive x-ray spectrometry (EDS) is advantageous for elemental confirmation. Using immunogold SEM EDS allowed us to ratify that our studies of FLO11p and surface adhesion was not a result of

artifacts of electron microscopy. We show that the cell strains with normal levels of FLO11p and knockout levels of FLO11p are unable to withstand the penetration of the 100-nm tall nanopillars, while the strain that overexpresses FLO11p could withstand the effects of the nanopillars. This was an unexpected finding as we predicted a linear response of deleterious effect to the expression levels of FLO11p. Findings of this study highlight the importance of surface topography when designing surfaces for microbial control, where surfaces can selectively promote or kill microbes based on their topographical features.

`

HIGH RESOLUTION VISUALIZATION AND CHARACTERIZATION OF CELL SURFACE ADHESION PROTEIN IN THREE-DIMENSIONAL NANOSCALE INTERPHASES

by

Reynaldo Thomas Díaz

A Dissertation Submitted to
the Faculty of The Graduate School at
The University of North Carolina at Greensboro
in Partial Fulfillment
of the Requirements for the Degree
Doctor of Philosophy

Greensboro
2018

Approved by

_____
Committee Chair

APPROVAL PAGE

This dissertation written by Reynaldo Thomas Díaz has been approved by the following committee of the Faculty of The Graduate School at The University of North Carolina at Greensboro.

Committee Chair _____
Dr. Dennis LaJeunesse,

Committee Members _____
Dr. Hemali Rathnayake.

_____
Dr. Jianjun Wei.

_____
Dr. Joseph L. Graves, Jr.

_____
Date of Acceptance by Committee

_____
Date of Final Oral Examination

ACKNOWLEDGEMENTS

For this work, I would like to thank my advisor Dr. Dennis R. LaJeunesse for being a great mentor throughout my Ph.D. program. I would like to thank the members of my committee for their time and recommendations as well. This work would have not been possible without Dr. Todd Reynolds Lab who provided us with the different yeast strains used in this study. I would like to thank the financial support of the T4 STEM outreach program, and JSNN.

I would be remiss to not thank lab colleagues these include Rackyapan Chandran, Kyle Nowlin, Adam Bosseman.

I would especially like to thank my family for being my pillars throughout this process.

TABLE OF CONTENTS

Page

CHAPTER

CHAPTER I

INTRODUCTION

The Elephant in the Room

> Four blind persons were placed in a room with an elephant. Unfamiliar with the animal they used their hands to try to understand the creature. The people who were blind relied on touch to interpret their surroundings. One of them was holding the trunk, they said it must be a serpent, while another one holding the ear believed it was a fan, one of the blind persons holding the tail said it was a rope, while the fourth placed their hand on the body and said it must be a throne.
>
> -Ancient Buddhist/Hindu parable

I begin this scientific document with an old proverb, a bit unconventional for a science dissertation. Yet, the above parable illustrates the importance of perspective when studying an unknown phenomenon, feature or structure. This parable carries well into nanoscience and microscopy, which is the focus of my dissertation. Like the blind person trying to understand the elephant, a microscopist constantly examines what otherwise would remain invisible. Diving into the microscopic realm at the nanometer scale is like deep ocean or space exploration, where an explorer may get lost in the vastness, a vastness, which can be seen in microscopy with every increment in magnification. In the words of Richard Feynman: "*There is plenty of room at the bottom."*

Let us carry this old parable further, by hypothetically shrinking our 4-meter-tall pachyderm roughly one million times to a size of 500 nanometers (500 nm). This is

approximately the size of a bacterium. Now the question is how can a scientist characterize this nanoscale elephant with the best microscopes available?

Although there is some overlap depending on the type of microscope, in order of magnification (from lowest to highest) the microscopes are: 1) A standard table top compound microscope, 2) Laser confocal microscope, and at 3) and 4) atomic force microscope and particle beam microscopes, which have similar levels of magnification and resolution.

A compound light microscope uses a series of lenses to multiplicatively magnify the light interacting with an object (reflecting or transmitting through the sample) to form an image. Although, a stereo dissecting microscope technically qualifies as a compound microscope, we can bypass this instrument as the magnifications typically top at 40 insufficient to capture enough light reflected off our 500-nm elephant. A compound microscope magnification capability ranges from 40 x to 600 x, with higher tier microscopes in the 1000 x, this is enough to roughly visualize this tiny elephant. However, we would not discern that what we were looking at was a miniature elephant; we would not be able to distinguish more than a speckle for magnifications under 200 x. At 400 x, an outline of the elephant may be distinguishable, but we would have a fuzzy shape. We may even notice that the elephant has some protrusions representing the trunk, the tusks, the ears, and the tail; but the exact nature of these extensions would be unknown and may even be artifacts caused by lens defects or aberrations. An important consideration is the focal plane, which is the two-dimensional area in focus and is partially defined by parameters of the objective lens. The focal plane can be considered

analogous to the palm of the blind person's hands in our parable, as the information obtained solely comes from the point where the hand is touching the elephant. A microscopist may acquire a more complete image of the elephant by collecting and combining images from different focal planes in a process known as stacking. However, there are issues with such approaches – how does one resolve one focal plane from another, let alone combine these images. Such limitations make distinguishing the features of a hypothetical "nano" pachyderm using a compound microscope impossible. Moreover, if the only perspective of this nanoscale beast was the top, a microscopist will be unaware that the elephant has legs.

A microscopist with a confocal laser microscope (CLM) will gather significantly more information of our hypothetical nano elephant. A CLM includes all the features of a compound microscope, but the uniqueness arises several optical tricks. One is the light source, a laser light of a specific wavelength that enables irradiating a sample with an intense and specific wavelength of light. The second is a pinhole aperture, which enables the illumination of only a single focal plane and the capture of light from this same focal plane during image formation. The third trick is the use of fluorescent probes to decorate only portions of the sample with this excitation and emission of a fluorescent photon, the observer targets and forms an image of incredibly specific interest aspects in the sample. If in our nano-elephant we added a fluorescent label that would target our the nano-tusks, we would discern the location of the tusks in our elephant. This technique can be repeated with different probes with different fluorescent properties for various aspects of our nano-elephant, which would allow use to recreate and image our nanoelephant, layer-

by-layer, section-by-section; fluorescent channel by florescent channel. This process of stacking allows us to generate a three-dimensional perspective. Although we will still be limited by the wavelengths of light and the depth of focus of our lenses, by using a CLM we can observe a live nano-elephant chewing or walking under our microscope. This live cell observation will not be the case for some of our other microscopes.

What if the observer wants to see greater details of this 500-nm elephant? What if the microscopist playing the role of the blind person in our analogy wants to see the hairs on the elephants back? Or the number of legs? Or the footprints of the elephant? As alluded above, optical microscopy is limited by its use of the visible spectrum of light by a physical phenomenon called diffraction limit, where the limit of resolution is roughly dictated by half the wavelength of light. Although recent development of a technique called super resolution microscopy enables resolve down to 20 nm point to point, using other tricks within probes (e.g. fluorescent probes that blink and then burn out) and sophisticated software to resolve fine feature. Yet, even with these newer optical techniques, it would be impossible to discern the hairs on the back of our nanoscale pachyderm. To make these types of observations a microscopist would have to leave the visible light realm - which seems to strengthen our original blind persons analogy -- and move towards the field of ultrastructural microscopy.

However, as we leave the realm of optical microscopy and the use of visible spectrum as our probe, the images that we generate of our elephant are no longer optical in nature, but mere projections or interpretations created by probing and stimulating our

sample with different energies. Although they appear as an image, the colors are a function of a computer algorithm generating the image (pseudocolor).

Atomic Force Microscopy (AFM) is an imaging technique that most closely resembles the blind person's hand interacting with the surface of the shrunken elephant. AFM works like a record player and uses a super sharp needle attached to cantilever to delicately probe the surface texture of the sample. All motion and movement of the cantilever is captured by a laser which interacts with the top of the cantilever; as the needle probe interacts with the surface atomic forces, the movement of the laser provides a feedback loop, extrapolating what the surface topography looks like down to the nanometer level. Besides generating an image of the surface of the back of our micro elephant, AFM allows the possibility of gathering information of other physical properties of the elephant's weight, and force. Despite the great magnification and resolution capacity of AFM, finer elements such as the legs, trunk, or tusks of the elephant would be difficult to visualize. Furthermore, the needle is spatially hindered and unable to probe beneath the elephant.

There is another type of microscopy within the same nanoscale resolution as the AFM. Particle beam microscopy enables nanometer scale observations and permits characterization of the underbelly of our nanoscale elephant. Particle beam microscopes are subdivided into two general types: scanning particle beam microscopes and transmission electron microscopes.

Scanning Particle Beam Microscopy (SPBM) generates a high magnification raster image using a beam of high-energy electrons or ionized atoms. However, to obtain

a micrograph, we need to prepare our nanoscale pachyderm using a rather intensive sample preparation technique, as data gathering is done under vacuum and bombarded with a high energy beam. This preparation process involves a chemical fixation, which is followed by dehydration, and the addition of thin layer of conductive metal to the nano-elephant before its introduction to the microscope chamber. The images obtained from SPBM often ultimately provide the greatest detail and the broadest view of the elephant. The underbelly of the nano-elephant may be observed by tilting the sample, so features that may have been unbeknown to the microscopist from the compound, confocal laser, and atomic force microscopy, would now be clear using scanning particle beam microscopy.

Transmission Electron Microscopy (TEM) has the highest magnification of all microscopic techniques. TEM often uses a higher energy electron beam to go through the sample, enabling up to atomic resolution, but the resolution limitation often lies in the sample preparation. As with SPBM, the sample must be chemically fixed and dehydrated, furthermore, TEM samples often require a staining, resin addition, and thin slicing. This thin slice is necessary as a sample thicker than 200 nm does not allow the transmission of electrons through the sample to reach the detector. A requirement to generate an image using TEM. The thin section makes it tedious to reconstruct the elephant's interaction with its surroundings.

Like in my modern reimaged metaphor, where the microscopist objective is to try to obtain the most accurate, detailed, and complete picture of a nano-elephant, much of the work that I will present is the effort to develop techniques to image and image a

world which we cannot directly visualize, that is the nanoscale world of microbes. My elephant is brewer's yeast *Saccharomyces cerevisiae*, and I act as the blind person gathering as best I can the full perspective of a single cell interacting with its surrounding nanoscale environment. Now I depart from this metaphor, which illustrated the challenge confronted when trying to visualize the microscopic world and helped introduce some of the techniques and definitions used for the exploration of the nanoworld.

Why Microscopy?

Since the mid seventeenth century, when Anton van Leeuwenhoek and Robert Hooke introduced us to the microbial realm (Gest 2004), microscopy has been a driving force for much of scientific progress. Microscopist are like pioneers motivated by a constant desire to uncover what seems invisible. Microcopy techniques have been so influential throughout the last century that they have earned Nobel prizes since the early 1900's up until modern day. In 1905, Robert Koch was awarded Nobel Prize in medicine for his microbiological work. Koch himself attributed that much his success was thanks to the Carl-Zeiss microscopes (Blevins and Bronze 2010). One hundred years later, microscopy has not become obsolete. Recently, the 2014 Nobel prize chemistry went to super resolution microscopy, and in 2017 the Noble prize in Chemistry went to cryoelectron microscopy. These honors demonstrate that microscopy withstands the tests of time. Microscopy remains as the most authoritative technique to observe and collect data at the micron scale and below.

The 2014 Nobel prize was in a type of fluorescent microscopy and the 2017 Nobel prize was in a variation of electron microscopy, both techniques are used to

visualize proteins with as much detail as possible. The determination of a protein's localization within the cell provides enormous information on the functionality of a protein, its requirements as well as the cellular responses and mechanisms in which a protein participates in the most direct manner. In my work, I image yeast cell/substrate adhesion through the Flo11 transmembrane protein without having to slice the cell or surface. Scanning particle microscopes are the best suited instruments for high resolution imaging of yeast cell wall-proteins in a whole cell. The wavelength of high-energy-beam electrons or ions is significantly smaller than the wavelength of light microscopes. Allowing to surpass the diffraction limit that challenges optical microscopes when trying to image nanoscale features.

There are numerous types of electron microscopes (EM) that use high energy electron beams to generate an image at a higher magnification. Every EM has different benefits and drawbacks. While atomic resolution can be obtained using cryo-scanning electron microscopy, transmission electron microscopy and scanning tunneling microscopy; these instruments render a two-dimensional micrograph and are challenged when trying to observe interphase interactions that occur in three-dimensions.

In terms of resolution and magnification, the SEM does not provide the highest detail possible among different microscopes. Scanning Transmission Electron Microscopy (STEM) has also been used to achieve higher resolution protein localization with immunogold (Loukanov, Kamasawa et al. 2010).

TEM studies use immunogold as the main workhorse for ultrastructural understanding of the cell. The drawback with TEM and STEM is the intensive sample

preparation required to render a micrograph. For example, to visualize biological microorganism a thin lamella of 200 nm or less (electron transparent lamella) needs to be prepared using an ultramicrotome or ion milling (Giannuzzi and Stevie 1999, Kizilyaprak, Bittermann et al. 2014). This thin slice entails intensive sample preparation, and will produce a two-dimensional image. For these reasons, the Scanning Electron Microscope (SEM) and Helium Ion Microscope (HIM) are the instruments needed to visualize the yeast-surface for a high magnification three-dimensional image. To confirm that we are visualizing the correct proteins we obtained chemical confirmation using Energy Dispersive X-ray Spectrometry (EDS) in mapping mode in addition to Backscattered Secondary Electron (BSE) localization.

To generate a three-dimensional image using a transmission electron microscope, multiple two-dimensional images need to be combined by changing the angle of collection, or stacking several sliced images (de Jonge, Sougrat et al. 2010). This is time consuming and labor intensive, rendering unsuitable for high through-put analysis. For these reasons, the best instrument for studying of microbes/surfaces or microbe/microbe interactions, is a scanning electron microscope (SEM) or a helium ion microscope (HIM), as both types of instruments will generate an image with high detail and resolution as well as three-dimensional quality with an appropriate depth of field.

Microscopy and Protein Localization

To understand how yeast cells, interact with their surrounding environment at the nanoscale, I developed a technique that enabled me to determine protein localization at the nanoscale on a yeast cell and obtain its spatial confirmation using a scanning electron

microscope equipped with energy dispersive spectrometry (SEM-EDS). The novelty of the technique lies in the resolution of the imaging and labelling cell wall proteins using SEM-EDS. EDS has been discouraged as a detector for volumes less than 1 μm^3. Furthermore, EDS is not ideal for heterogenous samples with a rough topography, as signal interference can occur with the complex topography. Previous reports discourage the use of probes less than 30 nm, as the antigens may be obscured by a layer of conductive coating. This is specially the case when the detection method is solely coming from an secondary electron image (Richards, Stiffanic et al. 2001). However, I developed a method that worked around these pitfalls.

I developed a method to obtain chemical and spatial confirmation at the nanoscale for a target of choice, the adhesion surface protein, FLO11p. I labeled the epitope tag of adhesion protein FLO11p found in *S. cerevisiae* with 20 nm gold nanoparticles (AuNP). I resolved the transmembrane protein FLO11p despite that it was adhered to rough nanostructured surfaces such as those found on the wings of cicadas (Morikawa, Ryu et al. 2016). Cicada wings (CW) have an evenly distributed array of nanopillars that contribute to the wettability which can range from hydrophobic to super-hydrophobic (Sung-Hoon, Jaeyeon et al. 2009) .

The Use of Immunogold and SEM

Since the late 1960's, during the early stages of SEM microscopy, the application of a thin metallic gold layer on a sample was used to enhance contrast and reduce charging (Boyde and Wood 1969). This practice is still in use to this day, usually a mixture of gold-palladium or gold-carbon is sputtered as a thin conductive layer over a

sample before imaging with particle beam microscopy. Sample charging is a result of a non-conductive sample being irradiated by the high energy primary electron beam and the local generation of excess secondary electrons (Bell 2009). Sample charging is presented as a glow in certain areas of the micrograph while other areas remain extremely dark. An example of charging can be seeing in ***Figure 1***. Charging produces artifacts in the image and limits the magnification and resolution attainable by the instrument. The application of a thin conductive layer allows the dispersion of charge and enables the escape of secondary electrons and backscattered electrons to the detector producing crispier, more detailed image. Gold has been used as a contrast agent in an analogous manner as osmium tetroxide or uranyl acetate is used to enrich the contrast in a monochromatic image within the cell itself (J. De Mey 1981, Hodges, Southgate et al. 1987).

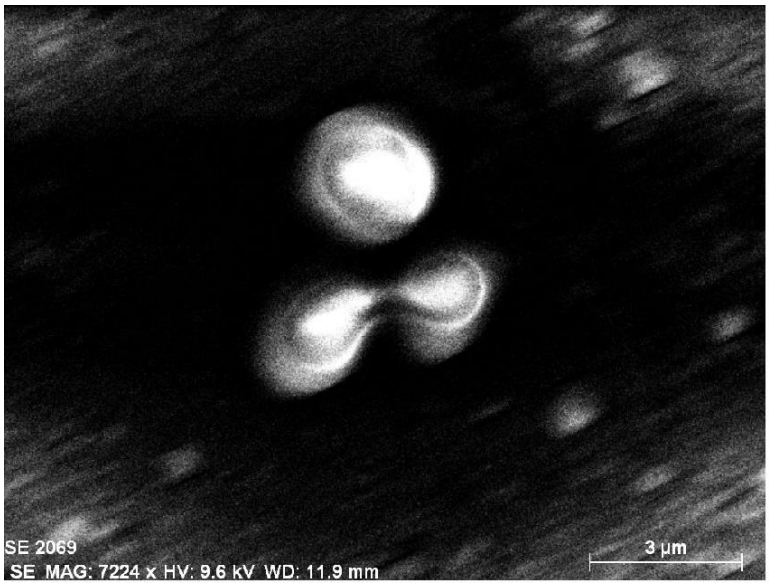

Figure 1. Charging. An example of the charging effect in an electro micrograph. Since no conductive coating was added to the sample. The sample is biological in nature,

generally making it non-conductive/insulator. Charging limits the detail a scientist can observe.

Yeast and Biofilm

We dive into the microscopic world to study yeast in the initial stages of biofilm formation. We are interested in biofilms as they represent an organized structure for unicellular organisms. The biofilm allows microbes to withstand stresses from the surrounding and proliferate in what the cell considers a hostile environment. Biofilms represent a major challenge in the biomedical world and industries that rely on biological processes such as the fermentation industry.

Antibiotic resistance is an ever-growing challenge in many fields. Biofilm formation is a key defense mechanism used by microbes to develop resistance to xenobiotics (Chandra, Kuhn et al. 2001, Nobile and Mitchell 2006). Biofilms are the sessile agglomeration of microorganisms in different environments either in solid-air, liquid-liquid or solid-liquid substrates (Costerton, Cheng et al. 1987, Simões, Simões et al. 2010). Biofilm formation presents a major medical challenge as it leads to highly resistant infections (Costerton, Cheng et al. 1987). Biofilms are linked to biofouling costing billions of dollars annually (Simões, Simões et al. 2010). Biofilms enhance the microorganism tolerance to environmental stressors and stimuli (Glinel, Thebault et al. 2012). To tackle biofilms, a lot of the focus has been on drug development that targets specifically the microbes or their extracellular architecture (Chandra, Kuhn et al. 2001, Simões, Simões et al. 2010).

Though biofilms are an enormous problem in some industries and communities, in other bioprocesses biofilms are sought after. Control and manipulation of biofilms and microbial flocculation is beneficial in microbial processes such as bioremediation or fermentation (Verstrepen and Klis 2006). Sewage water treatment plants rely on biofilms for steps in their treatment. Ethanol fermentation relies on yeast biofilms for a healthy process. (Hobley, Harkins et al. 2015) In beer and wine fermentation, depending on whether there is top or bottom fermentation, biofilms and cellulose scaffolding allow the yeast to have a competitive advantage over other organisms, it also enables better distribution of oxygen and other nutrients which improves product quality and yield (Fleet 2003, Servetas, Berbegal et al. 2013). Biofilms allow microorganisms to organize in a multicellular manner to increase their survival chances, which can have beneficial or detrimental effects on a system (Hobley, Harkins et al. 2015). Therefore, understanding, controlling and promoting biofilm formation is very important for many fields where any improvement will have a profound economic impact.

Cell-substrate adhesion is the critical first step in the formation of biofilms (Costerton, Cheng et al. 1987). Once a sessile cell anchors itself to a surface, the cell can reproduce and proliferate. The proliferation will create scaffolding, and remain adhered to a surface until it releases daughter cells for propagation or desorbs a whole piece of the film (Simões, Simões et al. 2010). The three-dimensional architecture of the pseudo organized cells protects the interior cells from being exposed to antimicrobial agents (Hobley, Harkins et al. 2015). Analogous to a herd of macroinvertebrate buffalos, enclosing their young in a circle to protect the heard from predators. Biofilms can be

composed of multiple types of microorganisms. Where yeast and bacteria can form a biofilm in a synergistic manner, thus benefiting both species. A common synergistic heterogenous biofilm can be seen in the popular drink kombucha (Jayabalan, Malini et al. 2010).

During the formation of stable adhesion to a surface the cell wall of the yeast S. cerevisiae is compromised when in contact with nanostructured surface (Nowlin, Boseman et al. 2015, Bandara, Singh et al. 2017). These early observations from our lab demonstrated that the nanostructured surface of the cicada wing of destroys *Saccharomyces cerevisiae* yeast on contact (Nowlin, Boseman et al. 2015). The compromised viability of the yeast is direct result of physical interactions with this nanostructured surface rather than a consequence from chemical toxicity. Other groups studying different microorganisms having found comparable results. Bacteria was compromised when interacting nanostructured surfaces (Ivanova, Hasan et al. 2012, Hasan, Crawford et al. 2013, Ivanova, Hasan et al. 2013, Pogodin, Hasan et al. 2013). These findings demonstrate a promising means, a purely mechanical means, of controlling a broad range of microbial biofilms without the need for chemical antibiotics. The control of microbial growth without the use of antibiotics reduces the potential of increasing the developing further antibiotic resistant microorganisms. However, the fundamental nature and dynamics of the mechanical interaction between the cell and the surface that results in a deleterious effect is not completely understood. We aim to determine the mechanisms that compromise the cell wall integrity when yeast interacts with surfaces of unique nano-topographies.

In my dissertation, I examined the role of FLO11p in the cell-substrate adhesion through high magnification particle beam microscopy. FLO11p is a cell wall protein that *Saccharomyces cerevisiae* yeast uses to adhere to surfaces or other cells. The hypothesis of my work predicted a linear deleterious response of the yeast when exposed to the nanostructured surface. I predicted that yeast cell with greater amounts of the cell adhesion protein (Flo11) would rupture more rapidly and efficiently in contact with a nanostructured surface such as that found on the dog day cicada wing, than those that had lesser amount. We also predicted that yeast cells which expressed greater amounts of Flo11 express phenotypes such as increased the stretching of the cell when interacting with nanostructured surfaces of higher aspect ratios.

Other research has looked at other parameters to study this mechanical disruption. A group compared different bacterial strains, including gram-negative vs gram-positive bacteria (Ivanova, Hasan et al. 2012). Another study took into consideration the role of cell hardness, and examined modifying the malleability of the cell wall by microwaving the cells (Pogodin, Hasan et al. 2013). The surface morphology has been examined as a variable to test their natural bactericidal effects, including dragonfly wings (Bandara, Singh et al. 2017), or nanopatterned surfaces (Li 2016). Yet, to the best of my literature search, the effect of adhesion protein (adhesins) have not been evaluated in these disruption dynamics. Since we know that bacteria and yeast rely on cell-wall proteins for intercellular attachment and adhering to different surfaces (Hori and Matsumoto 2010, Karunanithi, Vadaie et al. 2010), it is worth examining their role in this disruption. Gram-positive bacteria have a thick Pepto glycan layer while gram-negative have a thin

Pepto glycan layer as their outer most layer. Gram-negative bacteria tend to have pili in their cell wall that can act as adhesins, while gram-positive bacteria have pili, their function as adhesins remain uncertain (Proft and Baker 2009). In the study of Hassan et al. the researchers found that gram-positive bacteria had no reduction in viability (Hasan, Webb et al. 2013). The difference in survival between the types of bacteria was attributed to cell wall rigidity (Hasan, Webb et al. 2013). I predict that adhesins such as Flo11 are involved in the disruption dynamics. For this nanoscience doctoral dissertation, I investigate the role of a protein FLO11p in the rupture of S. cerevisiae yeast on natural nanostructured surfaces from the dog day cicada using high-resolution particle beam microscopy. In this dissertation I have covered the following aims:

AIM I: Determine *S. cerevisiae* viability and growth on nanostructured surface dependence on FLO11p expression. I compared the response of *S. cerevisiae* yeast with different levels of FLO11p expression when exposed to the cicada nanostructured surface using high magnification microscopy. We present a statistical technique for using microscopy to evaluate cell viability.

AIM II: We developed a technique for three-dimensional visualization of yeast cell-wall-surface-proteins using the Helium Ion Microscope (HIM) and immuno-gold SEM-EDS technique for submicron scale protein localization. We used immunogold coupled with EDS detector to confirm the location of FLO11p. We further ratified the location of the label using helium ion microscope and Scanning Electron microscope.

AIM III: Assess Nano Structured Surfaces NSS induced failure of cell wall *S. cerevisiae*. I used high magnification microscopes to zoom into the yeast and its surface contact points to assess current theories of cell wall failure analysis.

CHAPTER II

LITERATURE REVIEW

Microscopy

In the introduction I used a parable to quickly present microscopes with their benefits and drawbacks for studying the microscopic world and below. For this part of the review I will show how microscopy has remained relevant through time, further showing its importance using the Noble prize awards as an indicator of the recognition of the importance of the tool. I will present a quick survey of modern day microscopes with their capabilities and drawbacks. I will then focus on the Scanning particle microscopes, the instruments I most frequently utilized for data collection in this dissertation. To conclude the microscopy section of this literature review, I will present a literature survey of the use of immunogold as a protein label, to give a theoretical background for my work developing an immunogold EM technique.

The Importance of Microscopy through Time

Before microscopes, water filled crystals globes served as magnification tools, a practice dating back to the ancient Greeks (Singer 1914). Seneca wrote about this in his book *Quaestiones Naturalis*, where he advises to use water filled globes to make undistinguishably small letters appear clear and large (Singer 1914). Some of the early mathematics behind magnification can be attributed to the study of optics and refraction through curved mirrors presented in the works of Euclid and Ptolemy (Smith 2012).

Arab scientist Alhazen, in the X century utilized the refractive principles to project a magnified image of an object with several curved mirrors (Singer 1914). The first telescope developed in the XXVI century naturally paving the way for the development of the first compound microscope (Singer 1914).

It was in the XVII century that the importance of the microscope was cemented by the groundbreaking work "*Micrographia"* of Robert Hooke (Hooke 1664). Even though Hooke had a royal appointment, his work was catapulted by the contribution of Dutch lens crafter Anton Van Leeuwenhoek who had developed a technique for grinding very fine lenses and reluctantly allowed Hooke to use one of his microscopes (De Kruif 1996). Hooke coined the term cell when observing a cork slide, even though he was unaware that what he was observing was a microscopic organism. It was Leeuwenhoek who reported the first observations of a living microorganisms in a droplet of rain water (Gest 2004). As expected the ability to make microscopic observations propelled scientific progress then and continues to do so today. Scientific work focusing on microscopy may seem antiquated in the year 2018, yet it manages to stay as a cutting-edge field of research.

To gauge the scientific relevance of microscopy, we can look to the highest honor a scientist can receive, the Nobel Laureate. If we look at the prizes given since the inception of the awards, microscopy as a standalone technique has been awarded six times, two of which were in the last five years. There are an additional five awards that were not towards microscopy specifically, but their work heavily relied on microscopy. In chronological order the awards for microscopy were: 1) 1926 Chemistry.

Ultramicroscopy or dark field microscopy. 2) 1953 Physics. Phase contrast microscopy. 3, and 4) 1986 Physics. Split among two microscopic techniques, Transmission Electron Microscopy, and Scanning Tunneling Microscopy. 5) 2014 Chemistry. Super Resolution Fluorescent Microscopy. 6) 2017 Chemistry. Cryoelectron Microscopy. The list of Nobel laurate awards towards microscopy are presented in Table 1. I will go over these microscopes in the following section.

Table 1. List of Nobel Prize Awards Granted Directly to a Microscopic Technique. Information gathered from the Nobel Prize website www.nobelprize.org

YEAR	CATEGORY	AWARDEE	TYPE OF MICROSCOPE
1926	Chemistry	Richard Zsigmondy	Slit Ultramicroscope (Dark Field)
1953	Physics	Frits Frederik Zernike	Phase Contrast Microscopy
1986	Physics	Ernst Ruska	Transmission Electron Microscopy
1986	Physics	Gerd Binning Heinrich Rohrer	Scanning Tunneling microscopy
2014	Chemistry	Eric Betzig Stefan W. Hell William E. Moerner	Super-resolved fluorescence Microscopy
2017	Chemistry	Jeffrey Hall Michael Rosbash Michael Young	Cryoelectron Microscopy

While not specifically an award towards a microscopy technique, it is worth pointing out the Nobel prizes winners who are in great debt or contributed to the field of microscopy. Though under these criteria, the list could surpass to more than 20 Nobel laureates who have used microscopy in some aspect of their work. I have curated my list down to five, whose work I believe was tightly intertwined with microscopy. In reverse chronological order: In 2010 the Physics Nobel Prize was awarded towards the

experiments with graphene. The graphene single atom sheet was eluded though the use of Transmission Electron Microscopy (Meyer, Geim et al. 2007). In 2008 the Chemistry Nobel prize was awarded to the discovery and development of green fluorescent protein (**GFP**). A protein used as a label for fluorescent confocal microscopy (Kim, Truman et al. 2010), and it can even be used as a label in electron microscopy (Drummond and Allen 2008). The uses of GFP expand beyond the microscopy label, for which it makes it to this list and not the microscopy specific list (Tsien 1998). The 1974 Nobel prize in medicine was awarded for the structure elucidation and function of the cell. Much of the structure studies were performed using some of the first electron microscopes available, giving rise to the field of ultrastructural microscopy (Claude, Porter et al. 1947). In 1905 the Nobel Prize in Medicine was awarded to Robert Koch for his work on Tuberculosis. Koch was a huge innovator in microscopy, he was the first to publish an image of bacteria (Blevins and Bronze 2010), he was the first to use an oil immersion objective and made strides in sample preparation to examine under the microscope (Masters 2008). In 1902 the Nobel Prize in Medicine was awarded to Sir Ronald Ross, for his work in determining the transmission mechanisms of malaria. Though a lot of Ross work would be in the field of Public Health and epidemiology, his seminal work was done using a simple bright field microscope which observed the transmission of malaria from human to a mosquito (Ross 1897). This curated list is summarized in Table 2.

Table 2. Curated List of Nobel Prize Awards whose Work was heavily Based on Microscopy. Table gathered from nobelprize.org.

YEAR	CATEGORY	AWARDEE	DESCRIPRIPTION
2010	Physics	Andre Geim Konstantin Novoselov	Graphene experiments
2008	Chemistry	Osamu Shimomura Martin Chalfie Roger Y. Tsein	Discovery and development of Green Fluorescent Protein
1974	Medicine	Albert Claude Christian de Duve George E. Palade	Discovery concerning the structural and functional organization of the cell
1905	Medicine	Robert Koch	Work on Tuberculosis
1902	Medicine	Ronald Ross	Work on Malaria

Microscopy has been recognized as an important scientific tool since the time of the Greeks up to the most recent noble prize. A microscope is a technological tool that has enabled the development of entire fields of study. Now let us explore the modern microscopes, many of which were either conceived by or heavily influenced by the Nobel prize winners just mentioned.

Survey of Modern Microscopes

I will examine the technology behind today's microscopes. I do not intend to endorse any brand, but in some cases the microscopes are exclusive to a company. I will introduce the science behind these microscopes. Among light based microscopes, I will cover bright field compound microscope, confocal laser microscopy, dark field microscopy and some of the techniques that can be used with these microscopic setups to improve resolution and magnification. I will then proceed toward the particle beam microscopes. The common theme you will see in this survey are the capabilities of the microscope, the magnification, resolution, and the information beyond the image that a

scientist may obtain by using the instrument described. I will describe the mechanism behind signal generation.

Bright Field Compound Microscopes

The bright field compound microscope is the most widely used type of microscope, as most high school graduates will have to use it at one point in a biology class. It is portable and relatively affordable. The term compound is denoted from the multiplicative magnification of the objective lens and the eyepiece. The compound microscope is generally composed of a light, a condenser and/or aperture, a stage holder for a translucent slide, the objective lens, usually a prism and/or mirrors to direct the light to the eye piece or CCD camera.

The magnifications can vary by the combination of the objective and the eye piece. Typically, the eye piece has a magnification of 10x. The objectives can range from 4x up to 100 x. For objectives of 50 x and higher is necessary to use oil to avoid diffraction of the light travelling through different mediums, where the immersion oil has a similar refractive index as that of glass. The digital CCD camera enables a post-acquisition magnification; but should be considered just enlargement, even though the image may seem to have a higher magnification the resolution will not improve.

Lateral resolution or separation power is defined as the distance in which the full width half maximum of the intensity curves of two adjacent light points (Airy disks) can be separated (Bolte and Cordelieres 2006). In other words, the ability to differentiate between two pixels and is measured by the distance between the two pixels.

Confocal Microscopy

Also known as laser confocal microscopy, in terms of hardware the microscopes have similar components as the ones mentioned in bright field microscopy. The difference lies in the light source; besides the bright field this microscope has the capabilities of using different focused lasers. The use of focused lasers enables the use of fluorophores, which can be used as a label in immunohistochemistry. The resolution can increase significantly by the use of a pin hole aperture the size of one Airy disk that will filter out unfocused light (Bolte and Cordelieres 2006).

Within the Laser confocal microscopy, the resolution can be brought down to 20 nm, what is known as super resolution microcopy (Chemistry Noble prize in 2014). Super resolution is the result of optimization of sample preparation, data acquisition and post-acquisition reconstruction. Using specific molecule excitation and bleaching, a single marker can be pinpointed within a cluster of markers. With the use of total internal reflection fluorescence (TIRF) and photoactivated localization microscopy (PALM), the microscopist can increase the resolution down to 20 nm (Betzig, Patterson et al. 2006).

The last optical microscopy technique we will cover is dark-field microscopy. Which named appropriately the images generated seem to have a dark background, as it suppresses the angular unscatterred light from reaching the objective, which makes the micrograph appear to dark background (Hu, Novo et al. 2008). This technique was first introduced by Zsigmondy with his slit ultramicroscope that he used to observe the particles in a colloid (Zsigmondy 1926). Restricting the access of unscattered light,

increases the signal to noise ratio increasing the magnification capacity (Siedentopf and Zsigmondy 1902), though the blockage of the unscattered light can reduce the numerical aperture thus affecting the resolution (Harutyunyan, Palomba et al. 2010). Darkfield has the capabilities of visualizing plasmon resonance, a property found in rod shape gold nanoparticles (Alkilany, Frey et al. 2008) that allow for the optical examination of particles only 10 nm long (Siedentopf and Zsigmondy 1902, Zsigmondy 1926). The magnification and resolution an optical light microscope can attain is constrained by the diffraction limit which is dependent on the wavelength of the light and the aperture (Gustafsson 2001). This barriers were first introduced by Ernst Abbe Theorem (Köhler 1981, Breuer 1984), which without going through the mathematical derivations that use Fourier transformations roughly states the best resolution attainable is half the wavelength of light, approximately 200 nm for the visible spectrum (Zhang and Liu 2008). Using techniques like stochastic optical reconstruction microscopy (STORM) (Rust, Bates et al. 2006), photoactivated localization microscopy (PALM) (Fu, Huang et al. 2010), total internal reflection fluorescence TIRF (Reichert and Truskey 1990), capitalized by the super resolution work of Betzig et al can bring the resolution of optical microscopy down to 20 nm (Betzig, Patterson et al. 2006, Zhang and Liu 2008). Yet to surpass a 20-nm resolution limit of optical microscopes, smaller wavelengths like those used by high energy electron or ion beams are necessary to surpass the resolution boundary.

Particle Beam Microscopy

The Particle Beam microscopes use electron or ionized ions instead of photon to generate a signal. The particle beam microscopes can be divided into scanning particle beam microscopes and transmission electron microscopes A hybrid between the two microscopes is the scanning transmission electron microscopy (STEM). The main difference between these microscopes is the angle of detection of the signal. Where as stated by the name, the TEM and STEM operate like an optical microscope, where the electron beam will go through the sample. In the scanning particle beam microscope, the detector collects a signal bouncing of the sample.

The drawback with TEM and STEM is the intensive sample preparation required to render a micrograph. To visualize biological microorganism a thin slice of 200 nm or less, od an electron transparent lamella needs to be prepared using an ultramicrotome or ion milling (Giannuzzi and Stevie 1999, Kizilyaprak, Bittermann et al. 2014). This thin slice requires intensive sample preparation, and will render a two-dimensional image from electrons going through the sample. For these reasons, the SEM and HIM, scanning particle beam microscopy are the instruments needed to visualize the yeast-surface proteins on a plane for a three-dimensional visualization of the dynamics.

The two main microscopes utilized in this dissertation were Auriga Focused Ion Beam Scanning Electron Microscope with Energy Dispersive X-ray Spectrometry (FIB-SEM-EDS) and the Orion Helium Ion Microscope (HIM), both manufactured by Zeiss. The Orion has a field of view (FOV) that ranges from 1 mm down to 400 nm. The Orion HIM can achieve resolutions down to 0.23 nm (Notte and Goetze 2014), while the

SEM+EDS can achieve resolution of around 2.5 nm. For the high-resolution protein visualization using the HIM is great tool, as it provides greater depth of field and greater resolution (Notte and Goetze 2014). Figure 2 exemplifies the type of image produced by HIM versus SEM micrographs.

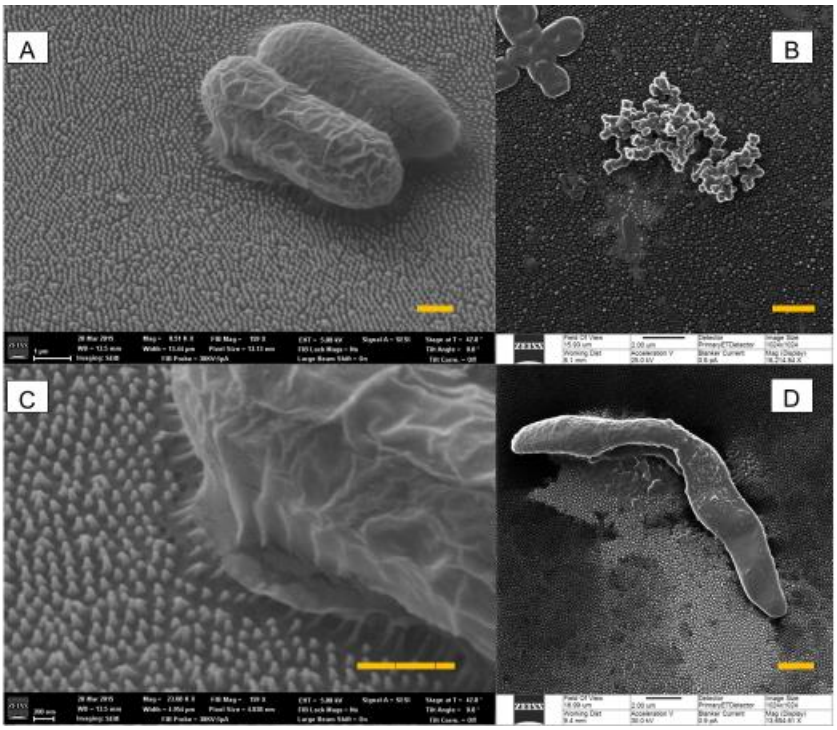

Figure 2. Shows the micrographs of the Cicada Surface Interacting with different Organisms. A) SEM image of wild type yeast adhering to the surface of the wing, in C) it can be observed that the cell wall is adhering to the nanopillars. B) HIM image of S. cerevisiae L6906 disrupted by the surface. D) HIM image of a fungi being disrupted by adhering to the cicada wing. Orange scale bar: (A, C) =1µm, (B, D) =2 µm.

Signal Generation

Both the helium ion and the scanning electron microscope follow a similar mechanism to generate a signal. Secondary electrons (SE) are generated by the energy loss that occur when an incident beam or backscattered electrons goes through a sample,

following the model Lenard type of adsorption (Kanaya and Kawakatsu 1972). Any SE generated from deep within the sample is usually reabsorbed and does not escape to the detector, this is why SE are considered more of a superficial signal (Klang, Valenta et al. 2013). backscattered electrons (BSE) are generated deeper from within the sample. The theory of BSE reflection is based on elastic scattering following either: Rutherford scattering, where the strong coulomb field of the nuclei deflects the incident beam (>90°); or as a result of multiple small deflections from the beam produces a reflection which is usually greater than 90° (Lloyd and Freeman 1991). BSE can be thought of as incident electrons that bounce back from the sample with an energy lower or equal than the incident beam. Depending on the voltage of incident beam, backscattered electrons signal intensity tends to increase with atomic number (Z) (Kempen, Thakor et al. 2013). This makes BSE suitable to differentiate biological elements from metallic gold label (Suzuki 2002, Kempen, Hitzman et al. 2013).

Despite of the magnification capabilities of the HIM, this instrument is best suited for fine etching. As an ion beam microscope, helium provides the smallest stable probe among all elements used for focused ion beams. Despite that the beam current is within the pico-Amps range, the sample will still damage if exposed for too long. The damaging effects by the beam can by either helium deposition (where the sample swells up) or by etching (where the sample seems to be burning away). As an etching tool, when compared to the established gallium etching, helium beam is analogous to using a scalpel to cut a sample versus an axe of the gallium source. This has provided wonderful use for nanomilling and nanoscale lithography.

The HIM has been used to make TEM lamellas in a similar fashion as a FIB would be used (Gregor Hlawacek 2014). The HIM has been used to mill 5 nm nanopores for the detection of biomolecules (Yang, Ferranti et al. 2011). The depth of these nanopores can be measured inside the scope by measuring the transmission through the sample being milled (Hall 2013). On nanofabrication the HIM has been used to pattern in graphene flakes with quantum dot devises (Kalhor, Boden et al. 2014). The HIM is likely establish itself as the go to instrument for nanopatterning in two dimensions for electronics and spintronics (Nanda, Hlawacek et al. 2017). As a lithographic tool, the HIM can provide an unsurpassed etch resolution since the SE emitted from the helium ion beam tend to have an order of magnitude lower energy (10 eV vs 100 eV) than those produced by e-beam etching. Higher energy SE will travel farther in the sample being etched, while the Helium etched will produce SE that stay near the beam (Melngailis 1993). The etching capabilities of he HIM is exemplified in Figure 3, which shows a chess board etched on a Si wafer, though overall this is not the outstanding image, it shows the sharp lines attainable using the HIM.

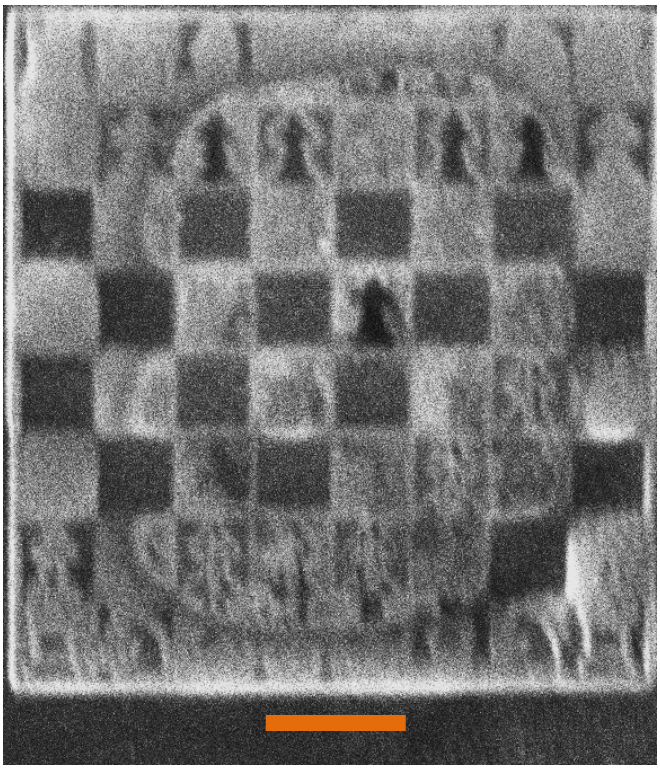

Figure 3. HIM Image a Chessboard on a Si Chip.

Better resolution and finer etching can be achieved by polishing the Si-wafer, adding a conductive coating and performing a plasma cleaning before patterning. The ring seen in the center of the board is an effect of sample burning/etching. A common risk when imaging with the HIM, for these reasons many opt to pattern with the HIM and image using an SEM. Orange Scale bar=500 nm.

EDS as an Immuno-Label Detector

The seminal paper by Fitzgerald et al in 1968 catapulted the use of x-ray dispersive spectrometry for material analysis in scanning electron microscopy (Fitzgerald, Keil et al. 1968). But it was until the 1980's that Hoyer et al used

characteristic x-ray to confirm two immuno labels in guinea pig hepatocarcinoma cells, one of these labels was gold (Hoyer, Lee et al. 1979). Due to the difficulty of the technique, characteristic x-rays was rarely included into the confirmation of the label where SE/BSE stacking was the preferred method (Hermann, Walther et al. 1996). This was before field emission became the main beam source for scanning electron microscopes which reduced the wavelength of the beam thus increasing the possible magnification attainable by a scanning/raster scope (Gounon and Le Bouguenec 1999). After which the use of EDS has had a comeback for material characterization in SEM, but not for whole cell immunohistochemistry analysis and usually limited to larger fields of view.

Obtaining quantifiable elemental readings from the EDS is challenged by complex topographies, as the topography of the sample can reabsorb the X-ray or photon hindering quantifiable elemental readings (Newbury and Ritchie 2013). In terms of data acquisition, EDS data can be gathered through point analysis, multipoint, line scan, mapping and hyper mapping. These acquisition approaches are presented in Table 3.

.

Table 3. Shows the different Data Acquisition Modes of SEM-EDS Analysis.

EDS Mode	Description	Advantages	Drawbacks
Spot (Single and Multi-spot)	Crosshair (s) select a location to focus the e-beam and generate a signal	Preview mode allows interactive live spectra readings	• Weak peaks • If charging occurs, drifting may give false reads
Line Scan	Drags the e-beam across a drawn line using pre-acquired image as reference	• You can observe changes in peak intensity in one dimension • Overall spectra give larger peaks	Hard to pinpoint exact location of element of interest
Mapping	Raster's the e-beam over a desired area, and provides pseudo coloring for elements. Color intensity corresponds to abundance of selected element at that point.	• Provides a spatial representation of elemental distribution • Provides approximations with low emissions.	• Low Peaks for Spectra • Time consuming, • Difficult to streamline

SEM-EDS technique reduces the sample preparation time and post data gathering three-dimensional stacking required in other microscopes like the Transmission Electron Microscopy (TEM) or Scanning Transmission Electron microscopy (STEM). The TEM and STEM coupled with an EDS detector can achieve higher resolution and elemental mapping due to the low volume interaction of the thin lamella or replicas used on these scopes (see Figure 4). In this work we show the characteristic elemental signature of a gold probe using the scanning electron microscopy using EDS to pinpoint the location of

FLO11p protein on the cell or substrate without the need of slicing or sectioning our sample of interest.

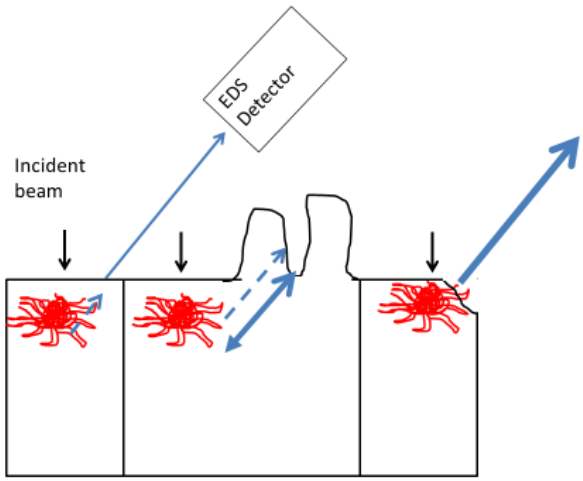

Figure 4. Cartoon shows the ways that the Topography can Affect the Signal. Where minimal interaction volume and a free path are ideal for EDS detection. Cartoon adapted from (Newbury and Ritchie 2013)

Even for microbial studies, where the interaction of S. cerevisiae with zinc, still had to resort to larger fields of views (50-100 µm) and a pelleted concentrated sample to obtain an EDS signal (Chen and Wang 2008). Still in larger FOV (200 µm) EDS was used to confirm the elemental composition of copper nanorods (Pandey, Packiyaraj et al. 2014). EDS is most useful for flat homogenous surfaces like semiconductors, where it can be used to confirm deposition or contaminants (Lu, Zhuang et al. 2011). We are interested in a smaller field of view and surfaces of varying topographies. As a rule of thumb, quantitative analysis EDS detection limit for a given element is around 0.1 % weight of the sample (Kuisma-Kursula 2000), the probe size still remains a challenge as it is within the 1 μm^3 when using the scanning electron microscope (SEM) (Echlin 2009,

GmbH © 2011 Bruker Nano GmbH, Berlin, Germany). Figure 4 Illustrates the concept of volume interaction and EDS signal. But it has been shown by Reith et al that it is possible to detect a gold nanoparticle on a bacterial cell using EDS, these were gold reduced by bacteria from solution (Reith, Rogers et al. 2006). The high concentration of gold in solution contributed to obtaining a large signal for the EDS analysis. To obtain a useful EDS reading, one should minimize the interference that may affect the path of the x-ray. Nevertheless, even with volume interaction, in mapping mode the coloration is not totally lost. These approximations are still very useful when dealing with spherical yeast, as the coloration is only a fraction of the cell. This can be used to determine the general region within the cell where the protein of interest is located where the immunogold is found

Immunogold for Electron Microscopy

At the beginning of the 1970's, the idea of using colloidal gold as an immuno label for salmonella surface antigens was presented for TEM analysis (Faulk and Taylor 1971). In TEM analysis, the gold label is readily identified as a particle that appears as a black spot on the image, a result of blocking the transmittance of the electron beam. In 1975, Hershberger et al, showed that 30 nm colloidal gold could be used a as a label for the SEM using only secondary electron (SE) detection (Horisberger, Rosset et al. 1975).

Gold nanoparticles are a great option for labelling since they have a high coefficient between secondary electrons (SE) and backscattered electrons (BSE), they are electron dense, and have a unique x-ray signal (J. De Mey 1981, Richards, Stiffanic et al.

2001, Goldstein, Newbury et al. 2012, Boyoglu, He et al. 2013, Orlov, Schertel et al. 2015).

The use SE for detection of gold nanoparticles is appropriate for probe sizes of 30 nm or larger, yet it becomes trickier when trying to detect smaller probe sizes as they are hard to discern from dirt or variations in the cell surface (Hermann, Walther et al. 1996). If a researcher wants to use a gold label smaller than 30 nm to have greater penetration to a desired cell, they may do so by later adding silver to the sample which enhances the size of the probe (Owen, Meredith et al. 2001).

The idea of using backscattered electron generated images to confirm the label was first introduced in 1981, where a secondary antibody was functionalized on colloidal gold to localize fibronectin (Trejdosiewicz, Smolira et al. 1981). Since then, stacking secondary electrons (SE) and backscattered electrons (BSE) to determine the location of a gold label has been the standard practice for immuno EM. To see examples of studies that use stacking of SE and BSE refer to the following: (Owen, Meredith et al. 2001, Richards, Stiffanic et al. 2001, Drummond and Allen 2008) as well as this work. For a review see: (Hermann, Walther et al. 1996). Even though gold label can be detected using the stacking of the SE and BSE to sub-nanometer resolution, as a standalone technique it is still prone to artifacts and user bias. Stacking SE and BSE for immunolocalization is still susceptible to error from other elements of higher atomic number that still may be present in the sample. To minimize potential artifacts that may arise, even with solid experimental controls, the staking analysis should be performed in

conjunction with detection of characteristic x-ray analysis and post-hoc size morphology analysis of the gold probe.

Gold has been used as an electron microscope protein labelling technique in many studies using microorganisms. (J. De Mey 1981, Hodges, Southgate et al. 1987, Richards, Stiffanic et al. 2001, Reith, Rogers et al. 2006, Drummond and Allen 2008, Castro-Longoria, Vilchis-Nestor et al. 2011, Boyoglu, He et al. 2013, Orlov, Schertel et al. 2015) For example, purified yeast nuclei have been labelled using a 10nm gold nanoparticles conjugated with a secondary antibody (Kiseleva, Allen et al. 2007). 10 nm AuNP have been used to label cellular organelles that were later imaged by backscattered electron (Drummond and Allen 2008).

Other Uses of Gold in Electron Microscopy

Gold is commonly used as sputtering agent to improve the conductivity and reduce the charging of samples being visualized by the electron and the ion microscopes (Wisse 2010, Lucas, Guenthert et al. 2014). The problem is that a conductive layer presents a confounding variable for the chemical identification of an immuno gold -tag smaller than 30 nm (Roth 1996). Therefore, we used carbon coating for our SEM-EDS analysis and the HIM to pinpoint the proteins on the cell surface, which will address the sample charging and not interfere with gold labelling (GmbH © 2011 Bruker Nano GmbH, Berlin, Germany). Gold has been used as a contrast agent in a similar manner as osmium tetroxide or uranyl acetate is used to enrich the contrast in a monochromatic image (J. De Mey 1981, Hodges, Southgate et al. 1987).

Immuno-gold is very useful for Transmission Electron Microscopy (TEM), it was first introduced in 1971 (Faulk and Taylor 1971). Scanning Transmission Electron Microscopy (STEM) has also been used to achieve high resolution protein localization with immunogold (Loukanov, Kamasawa et al. 2010, Peckys and de Jonge 2011).

Our research group is interested in the role of cell wall surface proteins interacting of nanostructured surfaces like the one presented in Figure 5. Since three-dimensional visualizing techniques of proteins at a nanoscale resolution are limited. The localization of this protein enables us to determine the dynamics of cell when interacting with nanostructured surfaces. In the SEM+EDS experiment we differentiate between yeast strains that have FLO11p with an HA epitope tag (L6906) with addition of the antibodies from yeast strains without the epitope tag or without the addition of antibodies. We labeled FLO11p with 20 nm gold nanoparticles (AuNP) functionalized with secondary antibody.

For our work we are investigating the dynamics of microorganisms with nanostructured surfaces (NSS). Our area of interest ranges from the 20 nm AuNP and up. As previously stated, to make observations in this scale we must use electron and ion microscopes, as optical microscopy highest resolution is of 20 nm (Watanabe, Punge et al. 2011).

Nanostructured Surfaces

The electron microscope sparked a resurgence in a naturalist drive to explore the surrounding with unprecedented detail. Scientist surveyed insects, plants, and inorganic materials to uncover whole new realms. Zooming into a surface thirty thousand times

revealed how the contours in materials can have so many variations. From an atomically flat graphene (Meyer, Geim et al. 2007, Lui, Liu et al. 2009), to the micro mountain ranges found in pitcher plants (Adams and Smithm George W. 1977), the diversity of structures seemed limitless. Before the electron microscope, it was impossible to achieve such high magnifications to appreciate the intricacies of these nanostructured surfaces.

Variations in morphology, distribution, and arrangement at the nanoscale change the overall surface energy of a material of identical chemical composition (Baer, Engelhard et al. 2013). These nanostructures will directly affect physical properties like wettability, light diffraction and strength (Bhushan and Chae Jung 2007). These nanostructures explained some of the puzzling properties of materials which have now embodied the field of nanoscience. For example, spider silk is stronger than steel and can pull water from air. The silk is natural nanocomposite, the strength is attributed to the molecular architecture of several protein crystals within an amorphous material. (Gosline, Guerette et al. 1999). The spider silk enhanced condensation property is due to the presence of periodic micro-knots within the strain (Zheng, Bai et al. 2010). One of the author's favorite examples is the club of a peacock mantis shrimp. This stomatopod's dactyl club is among the hardest and damage resistant materials, examining the club with SEM reveals it is composed of the chitin fibrils stacked in a helical arrangement (Weaver, Milliron et al. 2012). Besides being extremely tough, the mantis shrimp launches this biological hammer at such a high speed that it boils water and carries a force carrying a force of 693±174 N (Weaver, Milliron et al. 2012). Among the myriad of nanostructured

surfaces found in nature are: the gecko foot, shark skin, lotus leaf, the rose petal, and the cicada wing (Wegst, Bai et al. 2015, Zhang, Huang et al. 2017). Many scientist and engineers aim to replicate these nanostructured surfaces in their manufactured materials, an approach referred to as biomimicry. The way a material interacts with water is a frequent source of bioinspiration (Wen, Tian et al. 2015).

Wettability

Wettability is the property describing liquid-solid interaction (Li, Reinhoudt et al. 2007). The behavior of liquid-solid interaction was first examined seventy years ago, which correlated macroscopic aspects like apparent contact and roll-off angle with the surface features such as roughness or porosity. These studies led to derivation of the Casie-Baxter and Wenzel states (Cassie and Baxter 1944, Wenzel 1949). The surface wettability or water repellency is determined by the receding and advancing contact angle of water droplet with the surface. The substrate of interest is hydrophilic if the contact angle is less than 90 ° ($\theta<90°$). The substrate is hydrophobic if the contact angle is more than 90 °. A surface is superhydrophic if the contact angle is more than 150° (Li, Reinhoudt et al. 2007). Superhydrophobicity has been linked to resistance to sticking, fouling, and self-cleaning (Fürstner, Barthlott et al. 2005, Bormashenko, Bormashenko et al. 2007, Li, Reinhoudt et al. 2007, Xu and Siedlecki 2007, Liu and Kim 2014). This non-sticking property was sought after to avoid biological materials attaching to surfaces, but biomolecules' polarity involved in cell attachment vary significantly, making the development of a universal non-sticking material a major research hurdle.

A way to understand nanostructured is through its surface energy. This is usually determined by studying the surface interacting with liquids of known tensions (Bormashenko, Bormashenko et al. 2007).

Cicada Wing

In the LaJeunesse group what arose as naturalistic exploration using high magnification microscopes, developed into an unexpected discovery. Studying the cicada wings nanostructured surface, the scientists noticed that this surface exhibited antimicrobial properties (Nowlin, Boseman et al. 2015). The cicada wing translucent surface is composed of an evenly distributed array of nanopillars (micrograph in Figure 5). These pillars are approximately 200 nm tall and 50-100 nm wide. This wing pattern may present an evolutionary advantage as the wings are self-cleaning, water repelling and antireflective (Dellieu, Sarrazin et al. 2014).

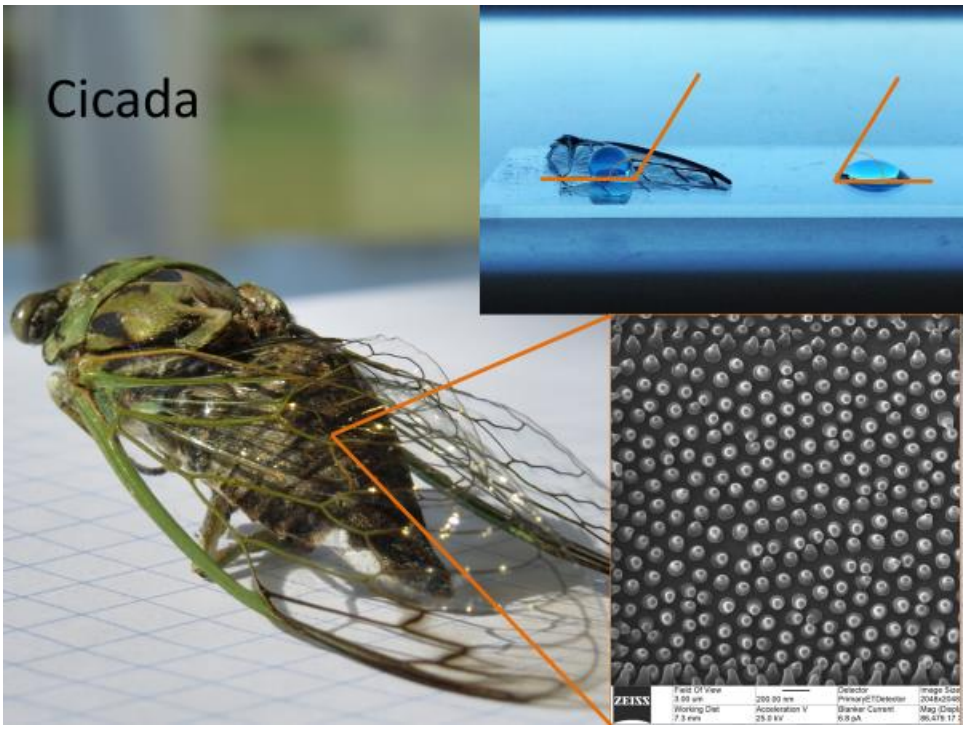

Figure 5. Shows the Annual South-Eastern Dog Day Cicada. N. *davisi.* Each grid measures 5 mm cicada. Top right shows the contrast between the contact angle of the cicada wing and a microscope slide. 20 µL of water were placed on the cicada wing and a microscope slide. Bottom left shows a Helium Ion micrograph of the nanopillars that constitute the cicada wing, scale bar 200nm.

Besides the unique wetting properties of the cicada wing, the LaJeunesse lab has found that the wing reduces cell viability of *S. cerevisiae* when trying to adhere to the wing (Nowlin, Boseman et al. 2015). This phenomena is a structure induced effect as modifying the surface chemistry still gave a reduction in the cell viability (Nowlin, Boseman et al. 2015). Similarly, changing the surface chemistry still had antibacterial effect (Hasan, Crawford et al. 2013).

The bacteria *Pseudomonas aeruginosa* has a reduction in viability when it comes into contact with cicada wing (Ivanova, Hasan et al. 2012) and as well as in dragonfly

wings (Ivanova, Hasan et al. 2013). Previously, superhydrophobic surfaces were believed to be self-cleaning thus impeding microbial adherence (Xu and Siedlecki 2007). But bacterial adherence those occur, and the nanopillars perforate the bacterial cell wall (Hasan, Webb et al. 2013). Synthetic materials like etched black silicon, with a similar roughness as the dragonfly wings, also resulted in a reduction of cell viability (Ivanova, Hasan et al. 2013).

The cicada wing inactivated gram-negative bacteria at 6.4×10^5 CFU cm^{-2} within 30 minutes of inoculation to a well plate containing the cicada wing sample, though for gram positive bacteria this group found no reduction in cell viability (Hasan, Webb et al. 2013). Gram positive bacteria survival was attributed to rigidity of the cell wall when compared to gram negative bacteria (Hasan, Webb et al. 2013). FDA disinfection guidelines for food safety evaluation was used to quantify the reduction in bacterial viability (Ivanova, Hasan et al. 2012). This test is based on extracting an aliquot of the suspension being incubated with the surface of interest to later perform a colony forming unit (CFU) analysis. This aliquot test would work if there was a chemical xenobiotic toxin being suspended in the solution, but the working hypothesis is that there is a physical disruption of the cell wall. The proposed mechanistic effect on these surfaces on the cell wall was presented by Pogodin et al in a paper where the bacterial wall is ruptured by the stretching occurring between the nanopillars (Pogodin, Hasan et al. 2013). Pogodin's et al free energy model potentially has the following flawed assumptions:

Cell wall thickness was not considered as it was one order of magnitude smaller than the nanopillars. 10 nm vs 70-200 nm. Cell wall thickness must be taken into consideration as this group has found that cell walls that are more rigid are not susceptible to the cicada wing disruption. As three gram-positive bacteria strains did not show a reduction in cell viability, where the gram-positive strains tend to have a thicker cell wall.

The curvature of the cell was not taken into consideration as it was several orders of magnitude larger than the nanopillars. The LaJeunesse lab takes into consideration that the whole cell is involved in the cell wall disruption response, as the rupture may occur as result of overextension of the cell wall, and the rupturing point might not even be in contact with the surface.

The interaction was strictly biophysical and there was no chemical or biological dynamics involved in the wall disruption. The LaJeunesse group is working on the hypothesis that adhesin proteins are heavily involved in the attachment to different surfaces, and this presents a highly dynamic system.

Treated the nanopillars as static rigid columns. We have observed that the nanopillars are not static, as when sampling trough electron and ion microscopy the rods move as a response to the beam energy. SEM micrographs show that the cell adheres to the nanopillars and can have different orientations as if the cells were pulling the pillars.

Independently from the studies of Ivanova and Pogoding, the LaJeunesse lab group found that the cicada wing was compromising the cell integrity of yeast *Saccharomyces Cerevisiae* for the yeast strains W303 and SK1. (Nowlin, Boseman et al.

2015). This challenges some of Ivanova's findings as the yeast cell wall is of higher complexity and varying rigidity when compared to the cell wall of bacteria. The cell wall of yeast rigidity can change depending on its surroundings stimuli (Levin 2011). This disruption is not purely biophysical and we believe that the adhesion proteins play a critical role in triggering such responses.

This moved the group's interest to the role of Flo11p. A well characterized protein found in the cell wall surface of S. cerevisiae yeast. We inoculated yeast to cicada wings to test for the effect of this adhesion protein. We hypothesized that the reduction in viability is a result of the yeast overextending itself while trying to adhere to a surface with a greater aspect ratio. This rupture of the cell wall is either a result of agitation while adhering to a surface, or the cell is retracting the adhesin proteins and overextending itself since it would be dealing with a high aspect ratio from surfaces like the cicada wing or the dragonfly wing.

S. Cerevisiae and FLO11

Saccharomyces cerevisiae is a great model organism, it is easy to culture and is one of the most extensively studied organisms presenting a solid theoretical foundation. *S. cerevisiae* genome was among the first sequenced (Winzeler, Shoemaker et al. 1999). *S. cerevisiae* has a profound socioeconomic significance just through its two main industries of bread rising and ethanol fermentation. Baker's yeast is very versatile, and continues to present potential applications in many areas of interest like synthetic biology. *S. cerevisiae* yeast has been used to tailor make a wide range of synthetic opioids (Thodey, Galanie et al. 2014), where the findings would be of great interest for

upcoming biopharmaceutical industry. For reasons like these, the enhancement of the understanding of adhesion dynamics and cell wall proteins of *S. cerevisiae* can be very beneficial to wide array of applications.

Understanding the adhesion of microbes to different surfaces is of extreme importance in many areas besides the biomedical arena. For example; bioreactors are compromised by bacterial adhesion to pipelines. Dentistry is a particular field which is interested in the bio-fouling resistant materials (Bowen, Lovitt et al. 2001).While promotion of adhesion is beneficial for areas where biofilms increase efficiency of a process. The beer industry looks after better flocculating yeast for beer clarity. This would cut cost of additives used for beer clarification (Dhillon, Kaur et al. 2012).

Yeast needs to regulate the flow of substance entering and leaving the cell as survival mechanisms (Teparić, Stuparević et al. 2004). In the case of *Saccharomyces cerevisiae* the interaction with its surrounding depends on the cell-wall proteins which act as sensors, that can trigger cascade responses depending on the environmental stimuli (Levin 2005). The regulation of the permeability of compounds and materials through cell-wall is essential in resisting osmotic changes in the environment. For example; when yeast adhere to a grape skin, it must be able to quickly adapt to a sudden environmental shock like a large influx of water like rain to not burst (Hohmann 2002). The cell wall of *s. cerevisiae* is essential to maintain the cell shape. In general it has to be rigid to protect against the environment, but it must be malleable to permit cell division, cell-cell attachments (Goossens, Ielasi et al. 2015) or pseudo hyphae formation during filamentation or starvation (Lo and Dranginis 1998, Braus, Grundmann et al. 2003).

Many of these response pathways are triggered by glycoproteins located at the cell surface which enable flocculation, adhesion, as well as other responses like maintaining turgor pressure (Levin 2005, Bou Zeidan, Zara et al. 2014).

Even though *S. cerevisiae* is generally regarded as non-pathogenic, it can give us useful insight into the mode of operation of pathogenic fungus like *Candida albicans* by the homologous adhesion protein family (Guo Bing, Styles Cora A. et al. 2000, Nobile and Mitchell 2006). *C. albicans* uses GPI anchored transmembrane protein to attach to epithelial cells (Sundstrom Paula 2002). Adhesion is a critical first step in biofilm formation in both bacteria and fungi/yeast (Chandra, Kuhn et al. 2001, Verstrepen and Klis 2006, Otto 2008). Cell-cell adhesion is essential for the formation of multicellular organisms. In yeast adhesion is necessary for the sexual reproduction and as an adaptive response to starvation (Braus, Grundmann et al. 2003). Starvation itself causes yeast to turn on the FLO11 gene, which promotes adhesion (Lo and Dranginis 1998, Braus, Grundmann et al. 2003, Bou Zeidan, Carmona et al. 2013).

The adhesion proteins in *S. cerevisiae* are known as the floculins or FLO proteins. FLO proteins are also involved in flocculation, hence the name. (Tofalo, Perpetuini et al. 2014, Goossens, Ielasi et al. 2015), FLO proteins play a role in yeast filamentation (Ryan, Shapiro et al. 2012), mat formation (Reynolds, Jansen et al. 2008), flor (Fleet 2003), and biofilm formation (Scherz, Andersen et al. 2014).

The expression of the *flo11* gene can present changes in the cell surface (Halme, Bumgarner et al. 2004). The FLO proteins are involved in cell-cell and cell-surface attachment. There are two types of dynamics in the current model of FLO proteins aided

adhesion, sugar-dependent and sugar independent (Verstrepen and Klis 2006, Bruckner and Mosch 2012). Flo1 (Miki BL, Poon NH et al. 1982, Kobayashi Osamu, Hayashi Nobuyuki et al. 1998), Flo5 (Tofalo, Perpetuini et al. 2014), Flo9 (Kraushaar, Bruckner et al. 2015) and Flo10 (Halme, Bumgarner et al. 2004) are proteins that bind to manosse ligands and require calcium in the process (Fleet 2003, Bruckner and Mosch 2012, Tofalo, Perpetuini et al. 2014); while FLO11p does not require mannose nor calcium for cell-cell or cell-surface attachment (Kraushaar, Bruckner et al. 2015). The mannose dependent N-terminal adhesins are likely not involved in the cell-surface attachment that lack lectins. Therefore, we are specifically interested in using FLO11 proteins as a variable in our cell-surface attachment study, since FLO11p can adhere in the absence or presence of mannose (Braus, Grundmann et al. 2003). FLO11p is a floculin protein of *S. cerevisiae* which is sugar/lectin independent (Lo and Dranginis 1998, Bou Zeidan, Zara et al. 2014, Sarode, Davis et al. 2014, Kraushaar, Bruckner et al. 2015), contrary to the yeast sugar dependent proteins involved in processes like adhesions to grape skin or ethanol fermentation (Fleet 2003). The expression *flo11* is necessary for the formation of mats on a semisolid surface (Reynolds, Jansen et al. 2008), mats are formed through the shedding of FLO11p, which is shed by cleaving its attachment to the GPI anchor (Karunanithi, Vadaie et al. 2010) . FLO11p is also correlated to pseudo-hyphae pathogenic invasion (Lo and Dranginis 1998). FLO11p is expressed in multiple yeast strains, (Bou Zeidan, Carmona et al. 2013, Bou Zeidan, Zara et al. 2014) but it can be solely expressed congenic strains descendent of Σ1278b strains (Lo and Dranginis 1998, Guo Bing, Styles Cora A. et al. 2000) where the Flo1, Flo5, Flo9 and Flo10 genes are not

active in these strains (Bruckner and Mosch 2012). Though FLO11 can also attach to mannose, we have chosen to use varying expressions of FLO11 to evaluate the effect of protein adhesion in mannose independent environment.

Flo11p crystal structure was resolved, the structure resembled that of fibronectin type III (FN3) structures, which is interesting since FN3 type proteins is typically found in the extracellular proteins of mammalian cells (Kraushaar, Bruckner et al. 2015). Further reinforcing the comparison of FLO11p with mucin (mucus) like proteins.(Karunanithi, Vadaie et al. 2010). There is FLO11-FLO11 homophilic and heterophilic interaction which was modeled to be pH dependent. FLO11A is the interest region of attachment and has an inside out topology like hydrophobins, though they might represent a whole new class of hydrophobins (Kraushaar, Bruckner et al. 2015). These interaction occurs between the aromatic bands found in FLO11A regions (Goossens, Ielasi et al. 2015), which was attributed to play a role in the hydrophobic interactions with surfaces (Guo Bing, Styles Cora A. et al. 2000, Verstrepen and Klis 2006). The waxy nature of the cicada wing and the chitin structure may favor the adhesion of the aromatic FLO-A region, thus enhancing adhesion of the yeast strains expressing the adhesion protein.

CHAPTER III

DETECTION OF IN SITU OF FLO11 PROTEIN USING IMMUNOGOLD LABELLING FOR SCANNING ELECTRON AND HELIUM ION MICROSCOPY

Background

In this work we use functionalized 20 nm immunogold to label cell-wall-proteins FLO11p, an adhesion protein found in Saccharomyces cerevisiae. We used immunogold for scanning electron and helium ion microscopes using secondary electrons (SE) and backscatter electrons detectors. The image generated by these two detectors is stacked and used as correlative microscopy, we are incorporating scanning electron energy dispersive x-ray spectrometry (SEM-EDS) for elemental confirmation. Chemical confirmation reduces artifact susceptibility. In this study we use EDS at the high magnification in uneven morphologies, a practice that has been discouraged due to volume interaction. The volume interaction of the EDS signal is of $1\mu m^3$, therefore examining a 5 µm wide yeast cell with the EDS detector generates noisy images with low peaks. We present suggestions to overcome the volume interaction barrier. We use nanoparticle gold (AuNP) as an elemental protein label. AuNP chemical signature is easily distinguished from the rest of the biological sample with EDS. Additionally, AuNP can be geometrically confirmed to corroborate localization. These techniques enhance the study of microbe adhering to surfaces and increases the through put of analysis capabilities of single cell electromicrograph analysis.

FLO11p Deposited on Aluminum Foil

Rationale

In this section we test the detection of the protein on a flat surface. As we examine the capabilities of using the HIM and SEM-EDS for immunolocalization, we must first set the baseline on an ideal flat topography to detect the protein. To enhance the contrast and minimize the coating we used aluminum foil. Aluminum provides an elemental background reference for the EDS detector.

Methods

L6906 yeast cells were grown to saturation and separated from the spent media. The spent growth media was then deposited onto the 5-mm wide aluminum foil discs as a dose and fresh YPD medium as a blank. EM sample preparation method was followed as described in the methods. We did not add a conductive coating to these samples. EDS analysis was done in mapping mode, we selected gold, and aluminum for the analysis.

Results

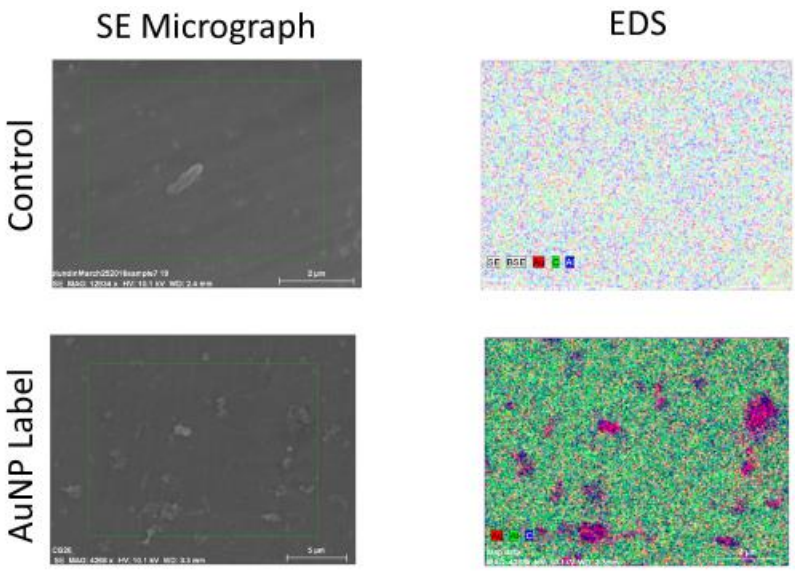

Figure 6. Contrast of the SE and EDS Mapping of the Gold antibody Label attached to the FLO11p with and without addition of gold nanoparticle.

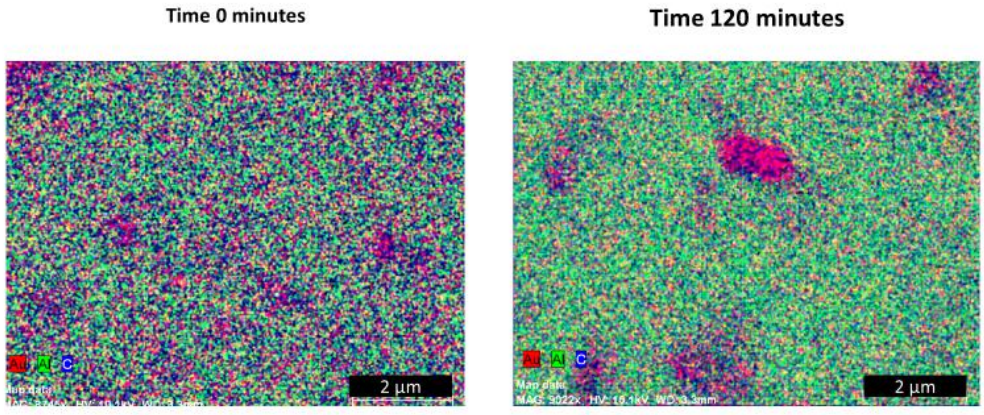

Figure 7. Comparison of detection between Initial Time Point and at 2 Hours

Discussion

Through the experiments of the immunogold labelling, we show that the EDS can be used as an immuno label SEM detector. FlO11p was deposited onto an aluminum foil to enhance contrast surface after a 2-hour incubation, a technique developed in the Resolving the transmembrane protein section. We tested the affinity of the secondary antibody with the 20 nm AuNP. As exemplified in Figure 6 there is a clear difference between the EDS image with the label versus the control.

Initially, this experiment was intended as time control experiment, we exposed the protein to the aluminum surface at different time intervals between a quick exposure (time zero) and two hours. We then added the immunolabel and examined the samples using SEM EDS. Figure 7 is a representative example demonstrating that we could not detect a significant difference between the two extreme points using SEM-EDS.

We successfully detected the gold label by itself on aluminum surfaces using the EDS and the SE detector. These experiments show us the ideal condition for detecting the immunolabel. This serves as an upper boundary reference from the immunolabelling for the whole cell. These readings serve as the baselines for detection of the immunolabel on the cell-surface interphase. As the topographies increase in complexity, the signal is expected to be lower due to the volume interaction.

Through these experiments we demonstrated that gold nanoparticle label does specifically bind to the primary antibody attached to the protein. As it was demonstrated through the protein deposition experiments, were we compared protein with primary

antibody but no secondary antibody with gold label to FLO11p with primary and secondary antibody with immunogold label.

Drop Casting Secondary Antibody onto Silicon Wafer and Copper Tape

Rationale

Most immunogold labelling papers localize the nanoparticle label by stacking secondary electrons with backscattered electrons. We compare the capabilities of detecting the gold nanoparticle using secondary electron detection, backscattered electron detection (ESB), and the EDS. We used unconjugated gold for this detection.

Method

We used 20 nm secondary gold antibody, and performed serial dilutions and drop casted them directly onto a silicon wafer with copper tape. We followed the EM sample preparation protocol, but did not add a conductive coating for the first sampling, but we then proceeded to add a 8 nm thick conductive coating for the second sampling. We used the copper tape to make an asymmetric guide for the drop casting.

Results

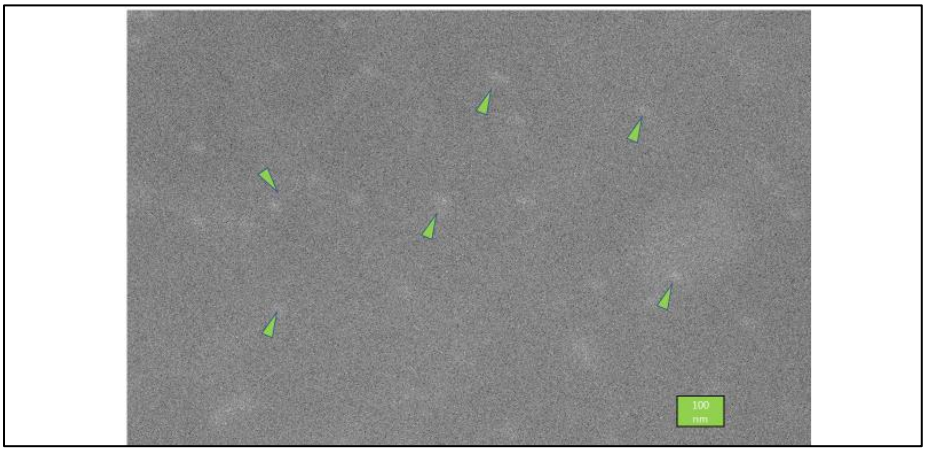

Figure 8. Micrograph collected with the Backscattered Detector of the AuNP, this sample has a conductive coating of 8 nm.

We were able to detect the 20-nm gold nanoparticle using the secondary and backscattered detectors. The nanoparticles were measured using ESB. The nanoparticles had an average diameter of 17.5 ± 2.3 nm without a conductive coating and of 31 ± 4 nm with an 8-nm conductive coating. Figure 8 is a representative micrograph of the ESB sampling. As addressed in the literature review the backscattered detector reduces the depth of field but is sensitive to higher atomic number elements like that of gold.

Discussion

These result show that we can detect the nanoparticle through a conductive coating using ESB and SE stacking. The measurements of the uncoated nanoparticle are close to that of the theoretical value of the nanoparticle. This additionally shows a radial increment of the particle measurement of 6.75 nm, which is within range of the expected coating deposition.

Using the EDS detector, we were also able to detect the label on a flat surface (Figure 9). We obtained a gold peak in the spectral analysis, in addition to the other reference peaks. This shows the ideal conditions for detecting the gold nanoparticle. Yet at this magnification the coloring is not as geometrically exact as the SE/ESB stacking. But it serves as a method to control for artifacts and is still able to localize proteins.

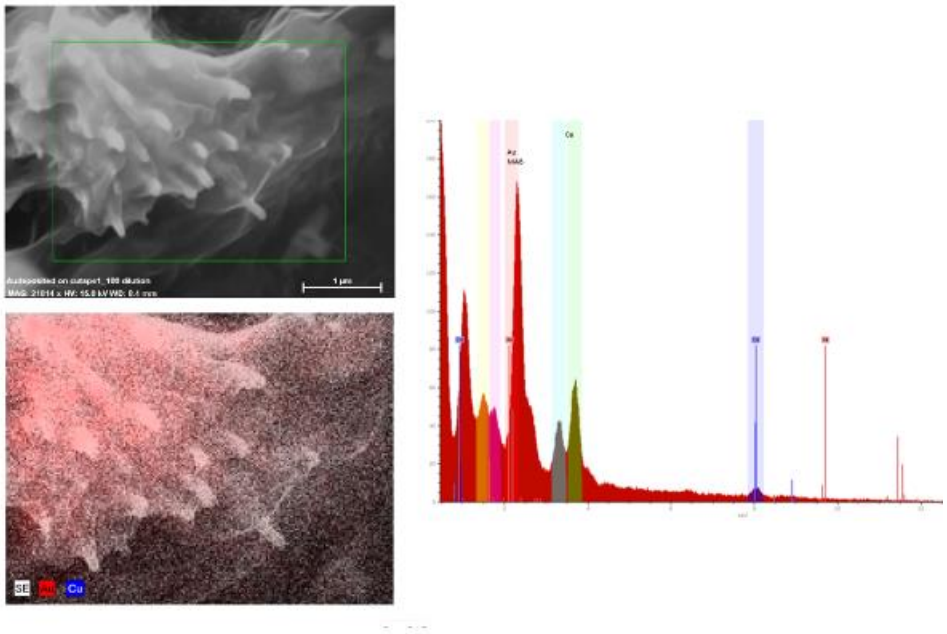

Figure 9. One Hundredth Dilution of AuNP. SE of suspected nanoparticles top left, bottom left shows EDS mapping mode image and the right is the EDS spectra.

Resolving Transmembrane Proteins with Little to No Coating

Rationale

A conductive coating generally sharpens and increases the resolution of a sample being observed by particle beam microscopy. Nevertheless, a 5-15 nm conductive layer can obscure noteworthy features when trying to resolve 20 nm protein labels. We explored methods to obtain a highly magnified and well resolved micrograph of the transmembrane proteins found in *S. cerevisiae* without the use of a conductive coating. We use the HIM which has a flood gun application that reduces charging. We used a highly conductive background/substrate to enhance the contrast of the uncoated yeast. We also examined the uncoated sample with the SEM-EDS.

Methods

We grew the strains TBR1, TBR4, TBR5, and L6906 overnight in YPD medium. We followed EM sample preparation protocol, without the addition of a conductive coating while following the yeast culturing protocol.

Results

Figure 10 shows characteristic uncoated samples of the different yeast strains. Though this technique is not recommended for accurately localizing proteins as it is apparent from micrographs presented in Figure 10. To acquire these images, the field gun potential and the grid voltage were adjusted. The contrast was enhanced using a metal background. As it can be seen in L6906, the lower the number of cells the better the resolution is. Though L6906 had the AuNP added, which can enhance contrast. As well

with no conductive coating, we localized the region on the cell using SEM EDS. This is exemplified in the micrograph shown in Figure 11.

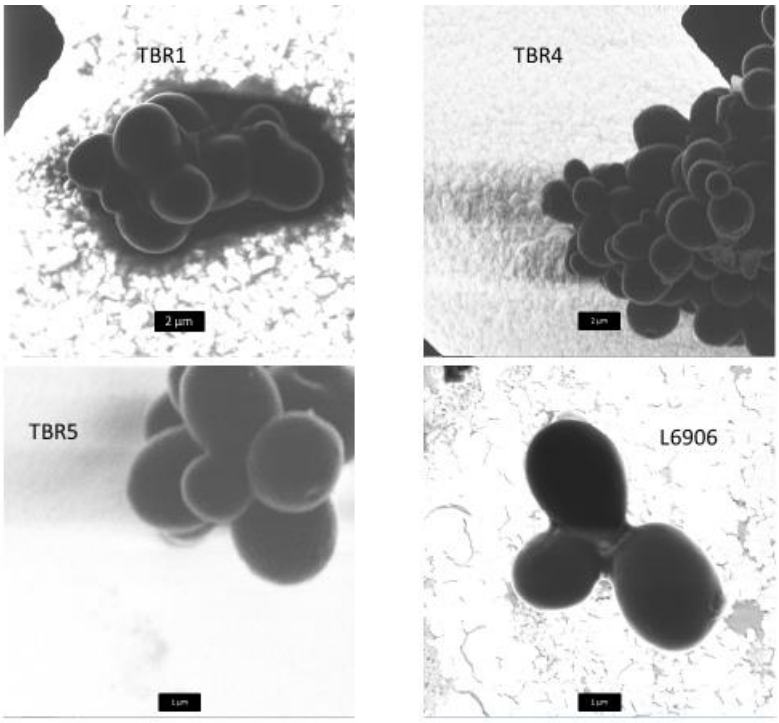

Figure 10. HIM images of the different Yeast strains Without a Conductive Coating.

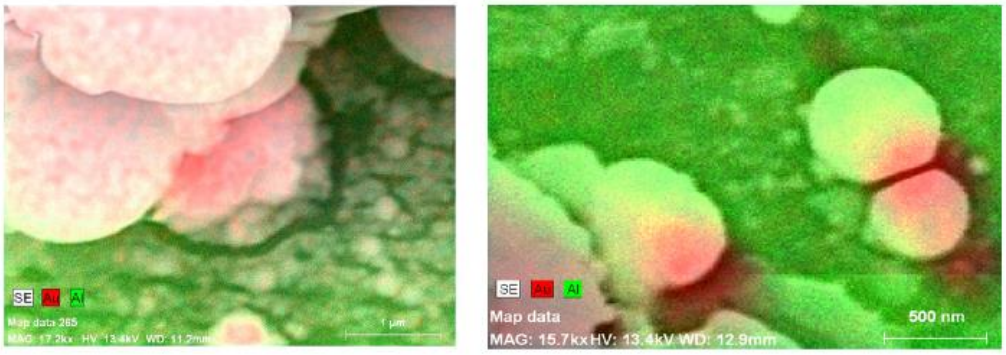

Figure 11. Micrograph of L6906 with Immunogold Label on FLO11p, but no conductive coating.

Discussion

Many of these experiments were designed to improve the imaging capabilities of uncoated microbes at high magnification. We were set on resolving and discerning the transmembrane protein FLO11, we omitted the addition of a conductive layer for two reasons. 1) The addition of a conductive layer could bury the protein of interest, and 2) the gold-palladium mixture can represent a confounding variable when looking for a gold nanoparticle with EDS. The EDS work gave a general sense of the region of the cells were FLO11 can be found. We saw that the gold label was localized near the bud scars of the yeast, at focal adhesion points between the yeast cells and other cells and substrates. This localization of the uncoated FLO11p with the SEM-EDS agrees with the extensive research on FLO11p, and other experiments presented here were a conductive coating was utilized. A common selling point for the helium ion microscope is the potential of making biological observations of uncoated samples. We were able to make such observations of microbes, yet with limited resolution. It is noteworthy the technique utilized to achieve the magnified images like those presented in Figure 10, where we used a highly conductive substrate as a background contrast enhancer of the insulating sample.

Detection of Gold Immunolabel using SEM EDS

Rationale

We use immunogold with EDS for the chemical confirmation of the localization of FLO11 protein on *S. cerevisiae*.

Methods

S. cerevisiae growth and maintenance

The L6906 strain of yeast was provided by the Todd Reynolds Lab group which has an HA epitope tag. Prior to any exposure experiment, one colony from the L6906 plates was suspended in 10 mL of YPD medium with streptomycin. After overnight growth in liquid medium, the culture was resuspended and diluted in fresh media to an optical density OD of 0.1-0.2. The cells grew again for two to four hours before seeding them onto a surface of interest, or conjugating with immunogold depending on the test.

Immuno gold labelling

As illustrated in Figure 12 and described in greater detail in (Goldberg and Fiserova 2016), the process of tagging FLO11p onto the cells consisted of the following: Live cells were pelleted at 400 rpm for 15 mins, later three times resuspended in PBSx1. The cells were fixed with electron microscope fixation solution (4 % paraformaldehyde and cacodylate buffer, at 4°C for 24 h. To minimize changing the surface morphology, or crosslinking the HA-tag, we used the immersion fixation recommended for microbes sample preparation in scanning microscopes (Russell and Daghlian 1985). The fixation solution was chosen since it is least destructive towards epitope tags (Murtey 2016). After fixation, cells were blocked with BSA, washed with PBSx1, (1^{ry} antibody was

added α-mouse in PBSx1 with 1 % BSA-ON/4°C). Added 2^{ry} antibody with gold nanoparticle 20 nm (1:100 dilution). After secondary antibody addition the cells washed once more with PBSx1.

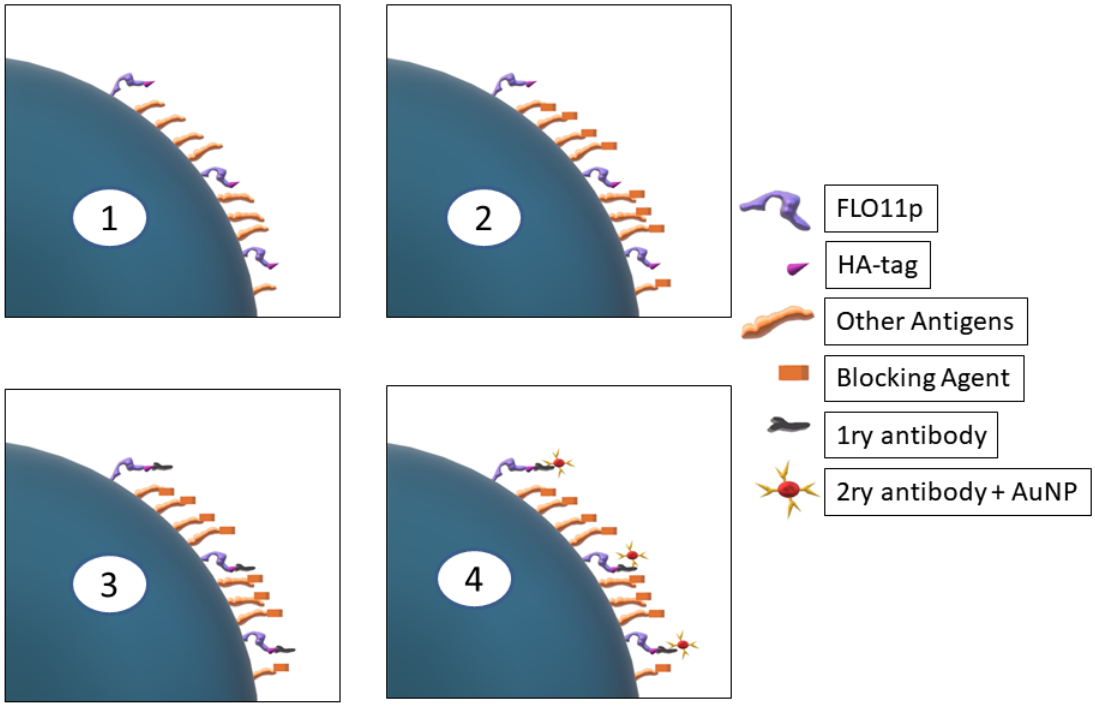

Figure 12. Scheme for Immunogold Labelling.

Figure 12-1. Show the cells with the triple HA epitope tag. Figure 12-2. Demonstrates the addition of the blocking agent used, the blocking agent utilized was BSA represented as an orange brick in the cartoon. Figure 12-3. Primary anti-HA mouse antibody was added, presented in the cartoon in black. Figure12 -4. Secondary anti-mouse conjugated with to a 20-nm gold nanoparticle.

As positive control, serial dilutions of the 20-nm gold nanoparticle were drop casted onto metal surfaces. We drop casted serial dilutions of the label itself onto

asymmetrical strips of copper tape allowing us to locate the dilution during imaging as spatial reference can be difficult to transfer into a magnified field of view. Aluminum and copper were selected to serve as background for parallel experiments. The metal substrates also enhance the immunogold probe (Owen, Meredith et al. 2001) and serve as an internal reference for the EDS analysis.

We also tested the affinity of the gold label towards FLO11p. Karunanithi et al demonstrated that FLO11 was shed to enable adhesion to surfaces or later aid in the formation of biofilm (Karunanithi, Vadaie et al. 2010). This work allowed us to assume that we could use the supernatant of the yeast medium as a FLO11p. We grew the L6906 yeast to a stationary phase and aliquoted the supernatant of the medium onto the aluminum surfaces and incubated for two hours with the suspension. The same incubation period used for the cells. We then followed the immunogold labelling procedure keeping an unlabeled sample as a negative control.

We optimized procedures like conductive coating, and excitation energy. We also set the baseline for particle size analysis. Additionally, we compared localization using SE, BSE and EDS readings.

Microscopy

The two main microscopes used were the Auriga Focused Ion Beam Scanning Electron Microscope with Energy Dispersive X-ray Spectrometry (FIB-SEM-EDS) and the Orion Helium Ion Microscope (HIM), both manufactured by Zeiss.

For the SEM-EDS metrology examination the conditions we followed were: SE as main source of detection, used a beam voltage of 5 kV or lower, the focus, stigmation,

and wobble were corrected on an adjacent parallel focal plane to the region of interest (ROI). Brightness and contrast adjustments were left automatic. The working distance was usually kept at 8 mm and no tilt was applied to the sample puck.

For Backscattered image acquisition, the beam voltage was kept at 4 KV or lower, the working distance was reduced to 4 mm, and a grid voltage was applied to filter out SE. For the EDS measurements, the working distance was kept around 8 mm, and the beam voltage was increased to 10 KV or higher to generate enough of a signal of the immunolabel. For most of the experiments, the samples were coated with an 8-nm carbon layer using the sputter coater to increase sample conductivity and reduce charge. Carbon was chosen over gold-palladium coating to reduce a confounding signal when trying to locate the gold nanoparticle. A set of experiments examined the addition of a gold-platinum layer to test if there would be signal augmentation from the from the nanoparticle and gold-palladium addition. The conductive coat was omitted for the samples trying to locate the label without any additional layer.

The EDS uses a Brucker detector coupled to the SEM. The beam was parked when acquisition was done using point or multipoint analysis. The stage tilt ranged from 23° to 45°. However, the main gauge towards optimizing the sample collection conditions was the live signal count going into the spectrometer. When collecting the EDS samples using the mapping and hyper-mapping mode of acquisition, the elements selected for examination were primarily gold for localizing the nanoparticle. Additionally, silicon was selected as a reference for the experiments drop casted onto a silicon wafer. Aluminum as a reference for the experiments where cells or proteins were

above an aluminum foil, and carbon when the substrate was the cicada wing and the conductive layer was carbon.

For the helium ion microscope, samples were prepared in the analogous manner as they were for the scanning electron microscope. The scope requires building a source and forming a trimmer on a biweekly basis. For samples with little or no conductive coating, the beam current was reduced to below 1 picoamp by increasing the spot size and/or reducing the helium pressure. To reduce charging on low coated samples, the flood gun was utilized when acquiring data. The multi-channel plate (MCP) detector was used to detect backscattered helium ions BSI (Postek and Vladár 2008), that are analogous to the BSE of the SEM.

A key assumption for statistical analysis of variance (ANOVA) is that the samples are randomized in their dosage/treatment and sampling. To meet this assumption, we randomized the sampling with the HIM and SEM. Additionally, when collecting samples, we ran it in triplicates with a positive and a negative control where applicable.

The randomization for both scopes consisted of: Assigning a spot for image acquisition as a starting point and later move the beam by randomized movement in the x and y directions (pan). Randomization was done to minimize user bias when acquiring a micrograph. We started by selecting a point of the sample puck from the external motion controller, at a zoomed-out field of view of 500 µm. The column lens started within the center of the sample of interest. To assign the random x and y movement of the sample we used the function “fx=randbetween()” in Microsoft excel. This generated pseudo random negative or positive numbers for both x and y direction would then be used as a

translational factor for the microscope panning. The experimenter would verify the suitability of the location under predetermined criteria, verifying that whether there was suspected microbe or label on the display. If not, the area was recorded as null or empty. If the area displayed contained an entity of interest we proceeded with zooming into the area, adjusting the focus, stigmation and wobble to later capture the image. Sample evaluation was performed after image acquisition.

Post hoc image analysis

All post-collection image analysis was performed using the open source application FIJI (imageJ2) (Schindelin, Arganda-Carreras et al. 2012). To make measurements of any element in the micrograph, the scale from the image was used as a reference for any measurement within each image. The usual procedure for analyzing an image consisted on the following sequence:

- Adjusting the image to an 8-bit image.
- The contrast was enhanced.
- The threshold was adjusted, if auto threshold was used the yen preset was the used for auto threshold.
- Particle analysis was performed when possible, usually on a homogenous surface as with complex fields of views this can be more prone to mistakes.
- When the image did not allow for Automatic particle analysis, regions of interest (ROI) were analyzed using the segment tool and stored in the ROI management, to later be measured
- All table with measurement results were saved as CSV file for later analysis, filed under the same name as the TIFF image file.

Results

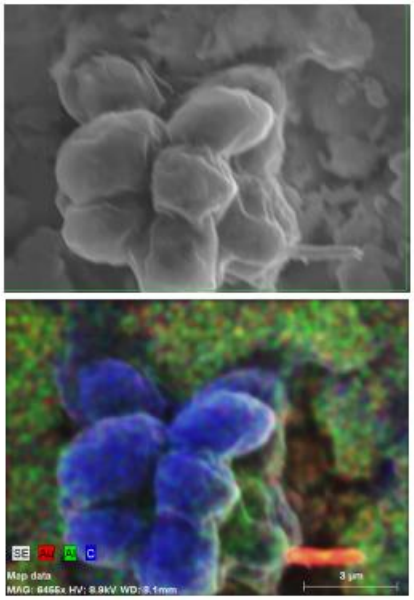

Figure 13. Shows and L6906 yeast Functionalized with Immunogold.

The top image shows the SE micrograph of the yeast above an aluminum foil substrate that was used as a reference. Bottom image shows the EDS map, with pseudo colored labels, where gold is red, aluminum in green and carbon for blue. Carbon was used as a conductive coating to increase magnification and resolution.

Discussion

Figure 13 is a representative image of immunolocalization using the EDS detector. The protein label is pseudo colored in red and be an extension coming out of the cell. This image alone visually confirms theories on the nature of FLO11 protein that state that the repetitive serine threonine regions can elongate, fuse and be shed for mat formation and adhesion to surfaces. With the immunogold label coming out of the yeast

cell wall in the mapping mode, we show that the intensity of the red color is a result of this protein being suspended and having low interaction with the aluminum foil surface enabling the escape of characteristic x-rays to reach the detector.

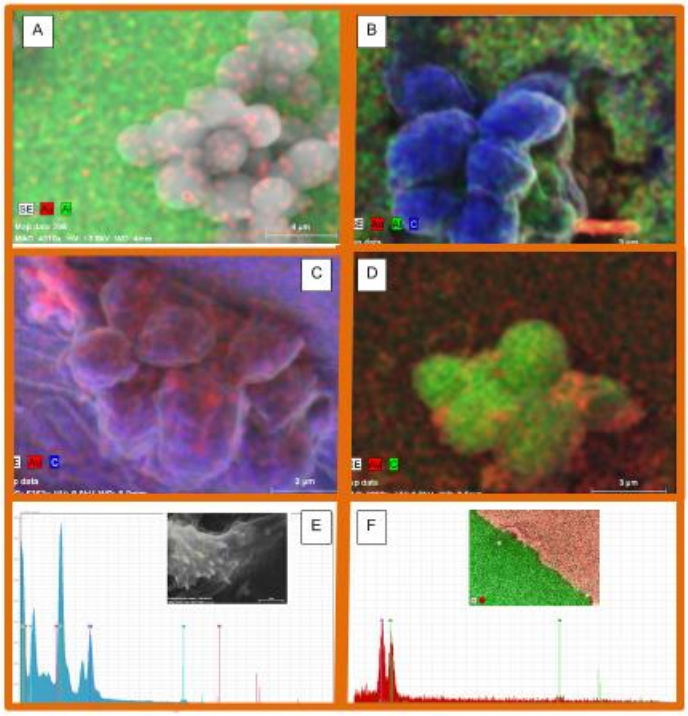

Figure 14. Different Gold EDS Detection. A) L6906+AuNP but no conductive coating on an aluminum substrate, scale bar 4 µm. B) L6906+AuNP with a carbon coating, scale bar 3 µm. C) D) L6906+AuNP on a cicada wing as the surface E) EDS spectra of 1 % gold dilution drop casted onto silicon wafer. Insert of SE image of the ROI. F) EDS spectra acquired from mapping a 100-nm thin coat of gold deposited on a wafer. Insert is an EDS mapping of the edge of the deposited gold.

The effect can be seeing as a sharp contrast of an extension (what we suspect is the FLO11 protein with the immunogold label) coming out of the yeast cell wall in the

mapping mode, we hypothesize that the intensity of the red color is a result of this protein being suspended and having low interaction with the aluminum foil surface. B and D.

The use of the EDS is challenging when dealing with volume interaction presented by the samples. Thus, it has been mainly encouraged for flat homogenous surfaces. Obtaining quantifiable elemental readings from the EDS is challenging due to the complex topography presented by the CW sample when irradiated with an electron or ion beam. The topography of the sample has a large effect on quantifiable elemental readings. Changing the tilt angle of the sample improves the signal. We have also see that we can reduce the scattering by limiting interference from the sample in its path to the detector in agreement with the literature (Goldstein, Newbury et al. 2012). Figure 14 show the importance of minimizing the interference of other elements when trying to localize the gold label.

Visualization of Yeast Cell-Wall-Surface-Proteins using the Helium Ion Microscope (HIM) and Immuno-Gold SEM Technique for Nanometer Scale Protein Localization

Background

This novel method that we are proposing takes 24 hours from start of yeast growth in liquid media up to finish when observing and collecting data in the electron microscope. Each step for sample preparation is a variable affecting the result, to which we had to optimize the sample preparation. We controlled for variables such as the ideal yeast inoculation stage and inoculation time onto a surface, and the optimal antibody kinetics. We minimized electron microscopy artifacts such as salt contamination by establishing sample washing protocol. The dehydration and fixing is necessary to observe biological

samples at high magnifications under the vacuum environments used with scanning electron/ion microscopes.

As reviewed in chapter II, the HIM can surpass magnification and resolution capabilities of the SEM. Following DE Broglie wave principles, using the helium ion in the probe reduces the wavelength of the beam thus increasing the magnification and resolution. Though both machines can achieve magnifications above the 60 KX, the HIM achieves these magnifications with greater ease, clarity, depth of field and topographical details. Here I am presenting a comparison of the SEM versus the HIM for immunogold localization using the EHT detector. We then compare both microscopes. These experiments are a good reference for comparison to the immunogold EDS work.

Methods

We used the yeast strain L6906 as our experimental unit and we dosed with the immunogold label and a control in a randomized fashion. We followed the EM sample preparation and examined under the HIM and SEM secondary electron detection. The error presented for these measurements is the standard deviation.

Results and Discussion

For high spatial resolution of proteins, the samples were examined through Helium Ion Microscopy (HIM), and Scanning Electron Microscopy. Using the technique of stacking SE and BSE we detected the label with the SEM (Figure 15).

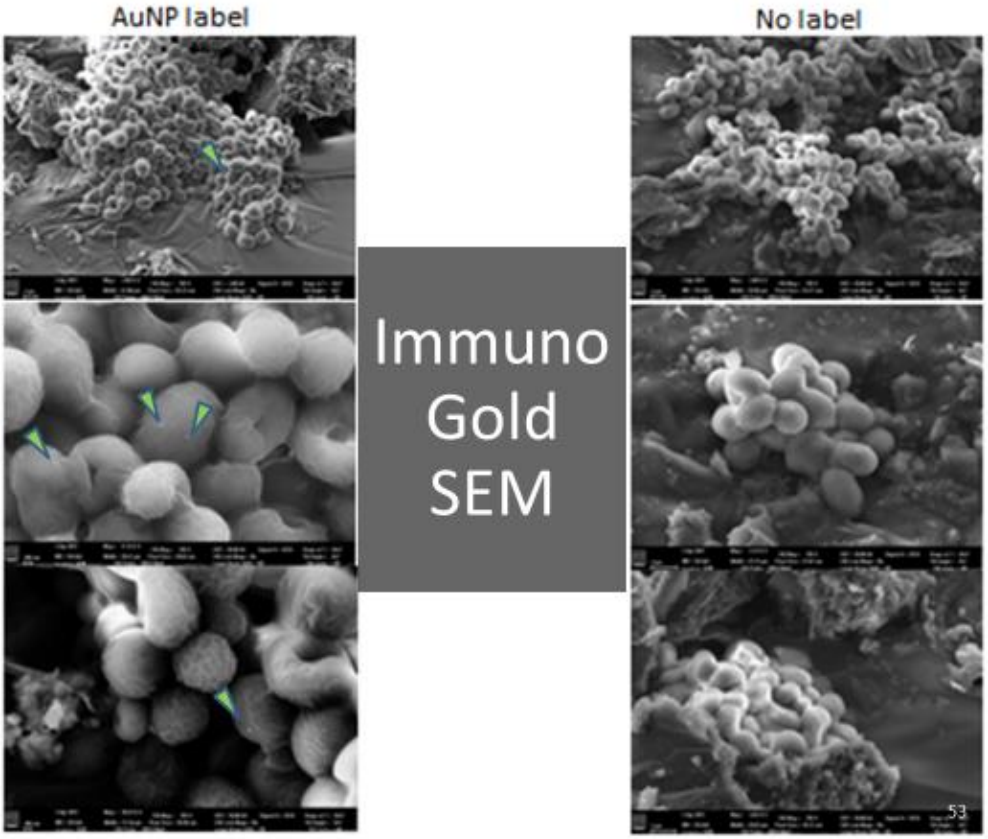

Figure 15. Comparison of Label vs Control of the Yeast using SE/BSE Stacking.

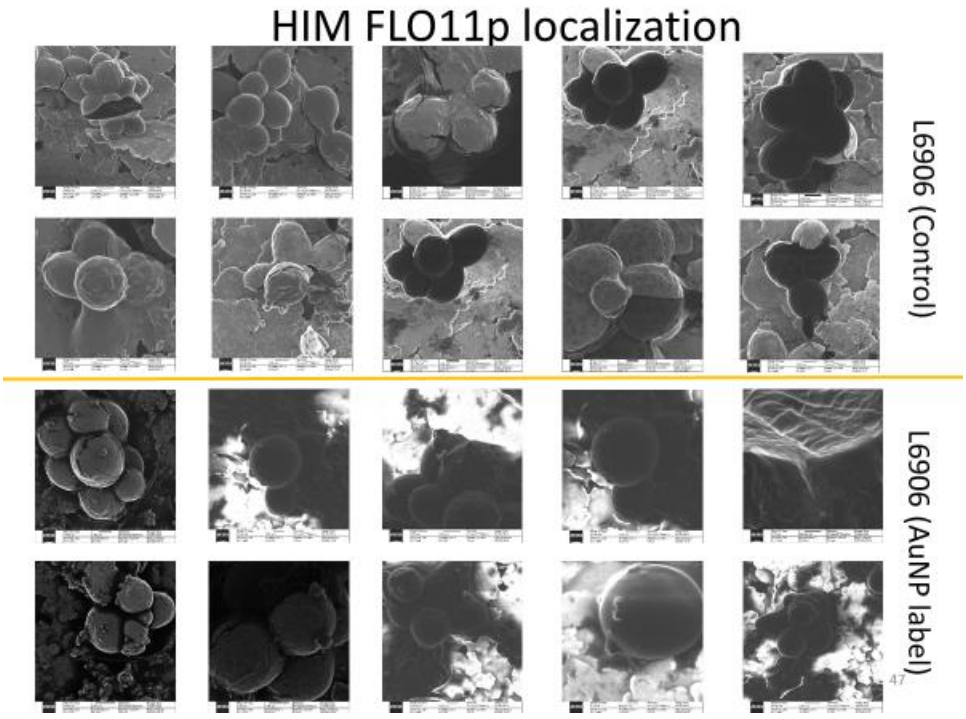

Figure 16. Images comparing the Immunogold using the HIM

We show that we can use the HIM to localize an immunogold label using solely the EHT detector, as it can be seen in Figure 16 and in Figure 18. Using both microscopes we could discern the labelled proteins from the control samples. Though for the SEM we had to use both the backscattered detector stacked with secondary electron detection. While for the HIM we could use only secondary electron detection. Throughout this document the reader can compare the micrographs of the SEM and HIM, but let us illustrate a general contrast by comparing the SEM micrograph in Figure 16 and HIM micrograph in Figure 18. Both images have the 20-nm gold label and a thin carbon coating. Even though the HIM image has a lower magnification, the reader can appreciate the greater depth of field presented by the HIM. In Figure 16, there is a small

depth of field, toward the front of the image, while in Figure 18 great details can be appreciated from different depth. Additionally, even though there still is some charging in the HIM image, the cell surface is clearly viewed, where the carbon coating can be seen flaking off the cell surface. While in Figure 16, the SEM charging does not allow visualization of the cell surface detail. It should be noted that the recommendations to visualize biological samples in the SEM are to use a lower voltage between 1-5 KV not the 10 KV used in Figure 16 to trigger the characteristic x-ray of gold for EDS analysis. For the immunogold labelling of FLO11p, the HIM resolved the label on the cells and substrates surrounding it. We localized and measure the probe size on the label with a thin coat of carbon Figure 16. This can be further exemplified by the micrograph in Figure 19, which shows a high magnification image of the cell surface and with tabulated results and the histogram distribution. Following suit for the different samples we detected the AuNP on substrates with a measurement of 81±42 nm on the cell. While the label on the substrate measured 25.8± 8.1 nm for this image. Considering the coat of 8 nm, we can state that the HIM can be used for an accurate measurement of the label but not very precise one. While the BSE particle analysis on a substrate gave an average size of 17.5 ± 2.3 nm without the use of conductive coating.

The difference between in the measurements of the nanoparticles on the surface with the label versus the nanoparticles on the cell wall, can be explained by the stoichiometry of the HA epitope tag.

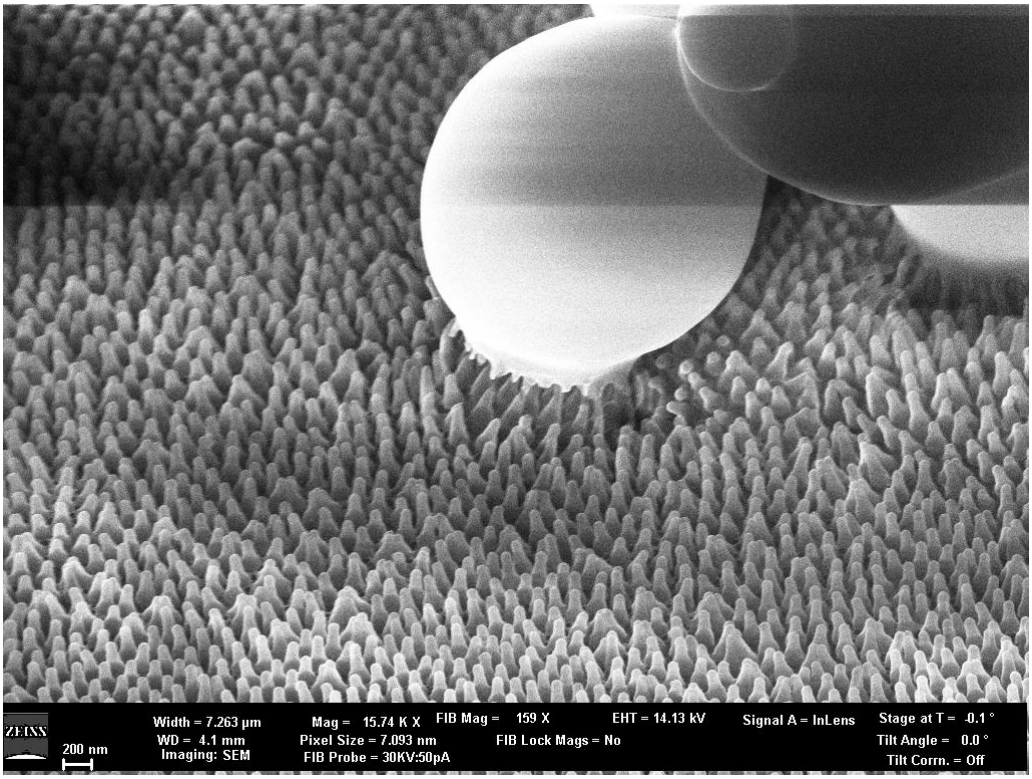

Figure 17. SEM image of L6906 Yeast Adhering to Cicada Wing NSS. The sample has a 3-nm thin carbon coating.

A reason for the difference can be attributed to the HA-tag itself found on FLO11p, which is a triple epitope tag, so there could be several nanoparticles attached to the protein, or the protein itself is concentrated in certain areas of the cell making the SE image of the tag look larger. We can corroborate that in fact what we are observing are the tags based on our controls in immunolabelling preparation, the unlabeled proteins did not show the suspected elements of the tag.

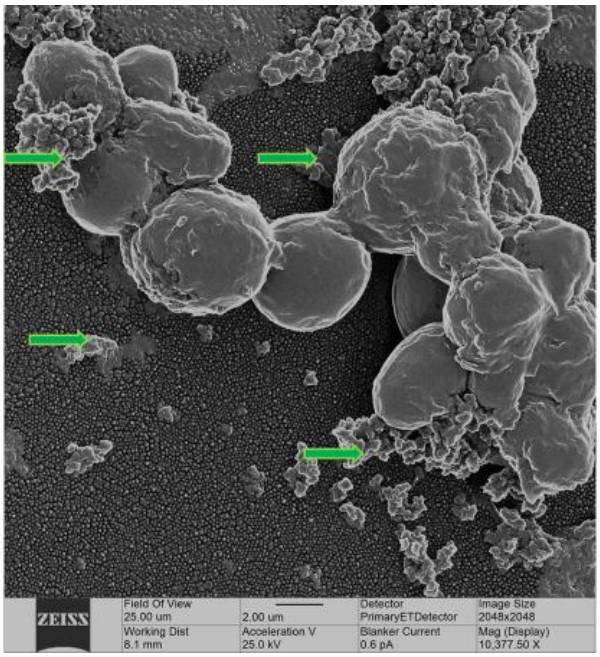

Figure 18. HIM Image L6906 Yeast with Primary and Secondary Gold Label.

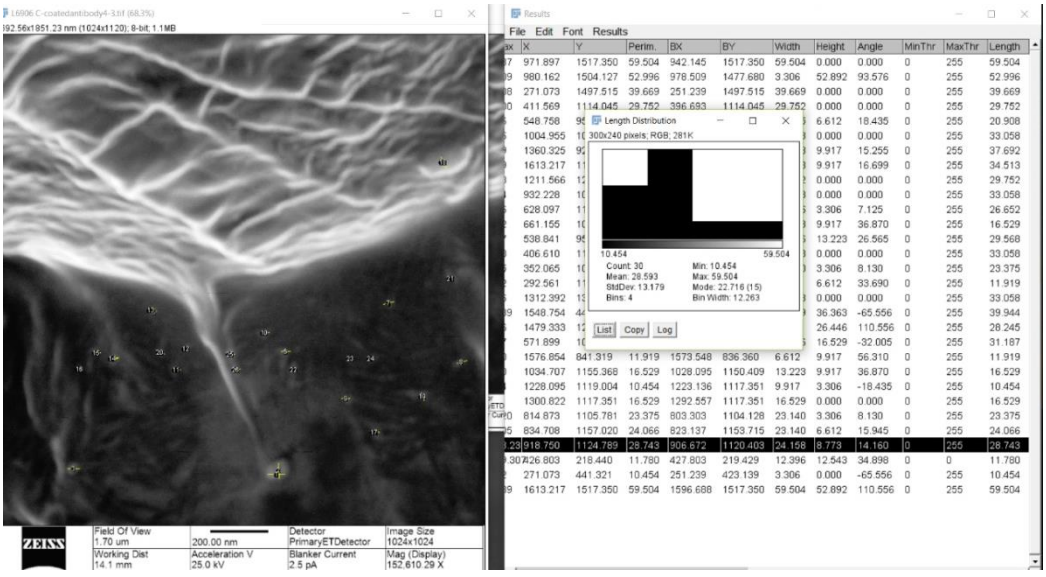

Figure 19. FLO11 on Cell Surface. This is a highly magnified HIM micrograph of the cell surface, top adhering to an aluminum surface. The FLO11p can be seen extending onto the surface. Despite the 5-nm carbon coat the 20nm AuNP can be detected with using only an SE detector. The label measured 28 ± 12 nm for this image, which taking into consideration the coat is an accurate measure of the label.

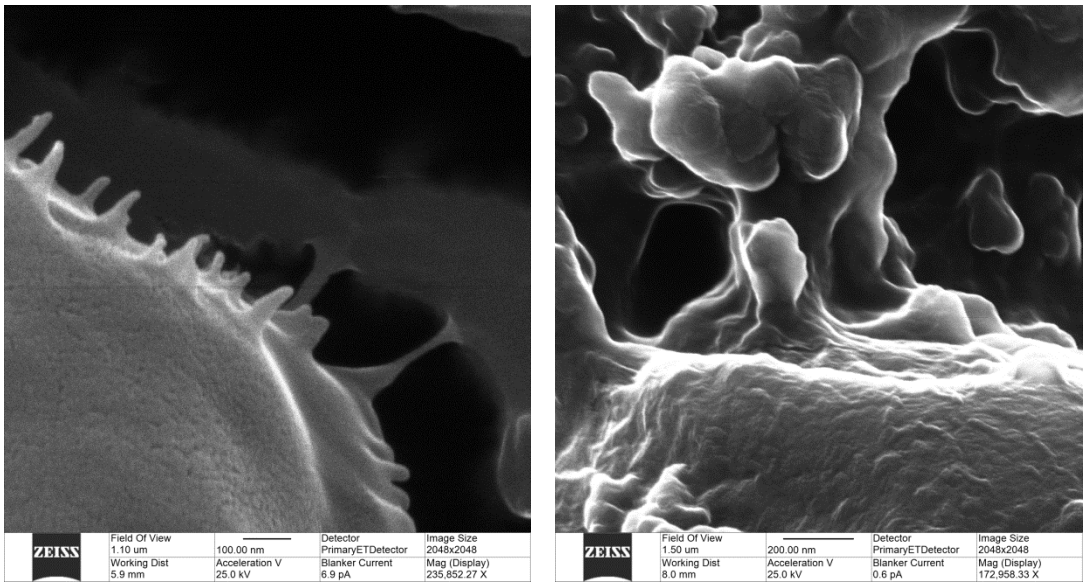

Figure 20. Image taken with the Helium Ion Microscope of Yeast Cell Surface. The cell surface proteins can be observed.

Figure 20 presents a highly magnified micrograph of the transmembrane proteins found in yeast cell wall. The left micrograph shows the TBR1 cell surface, the extensions coming out is what we suspect is Flo11p. Scale bar=100 nm. Right micrograph shows. Yeast L6909 on cicada wing coated with carbon. Magnified to 172 KX to show the adhesion protein. Gold labelled antibody was added before fixation, which shows a wider protrusion coming out of the cell wall. Scale bar = 200 nm.

The HIM remains as a scope that can achieve unprecedented magnification with a large depth of field in comparison with other scanning probe microscopes. That said there are a couple drawbacks presented by the HIM. A common user critique has been that the LUT acquisition transformation into a grayscale image is suboptimal. Experienced electron microscopist expect a micrograph to have rich gamma in the grayscales, yet the ones generated by the HIM tend towards darker black images

(personal communication at HIM user conference). It is common to see dark areas where there seems to be low SE emission, or plain absorption of the helium.

Chapter Summary

We show that localization of the immunogold nanoparticle is possible using the SEM as a detection method. We showed that the localization within a flat homogenous surface presents the best result for obtaining a signal from the nanoparticle label. We isolated the tag itself and on a flat and rouged surface. Additionally, we used Helium Ion microscope to pinpoint the location of the gold tag using an EHT detector to localize a 20-nm tag with an 8-nm coat of carbon at a very high magnification on the different surfaces. The limitation of the interaction volume that challenges EDS as a tool for immunohistochemistry in SEM can be circumvented by mainly changing the angle and varying the incident voltage on the sample of interest. Though the 20-nm gold label was not resolved as a particle using EDS, it is still a very useful tool for confirmation, since ultimately it is coloring the entire protein next that was intended for the labelling. An approximation of were the gold is expected to be located using the immunogold SEM labelling technique.

Conclusions

Adding EDS to immunogold analysis enhances the technique for protein localization as it can help overcome artifacts and potential errors in the analysis. Though the roughness of microbes interacting with a surface presents a challenge for the EDS detection as the escaping x-rays for elemental analysis interact with the uneven topography. We present suggestions to overcome the volume interaction limitation of 1

μm^3. Though we recognize that volume interaction is challenging, therefore cannot be used as a standalone technique. The use of BSE, post hoc size-corroboration of the nanoparticles, and EDS detector are not stand-alone techniques either but together provide a powerful tool for high resolution protein visualization. To obtain high detail surface protein micrographs the HIM was used to resolve the gold immunolabel. With the HIM we distinguish the 20-nm gold immunolabel using EHT detector for SE signal. Where the previous recommendation was to use 30 nm or greater nanoparticles for SE detection.

CHAPTER IV

ROLE OF FLO11 PROTEIN EXPRESSION ON *S. CEREVISIAE* SURVIVAL AND GROWTH ON NANOSTRUCTURED SURFACE

Background

In this chapter we present a method to quantify disruption in cell integrity directly on the surfaces using scanning particle beam microscopy. We examine the changes in cell morphology of S. cerevisiae with scanning beam microscopy. We study the effect of surfaces on the cell shape integrity while *S. cerevisiae* is trying to adhere to such surface. We initially hypothesized that adhesion plays a key role in the process that disrupts cell integrity, where much of the surface adhesion is a result of the transmembrane protein FLO11p. We expected that cells expressing more FLO11p would have a higher disruption in the integrity of the cell wall.

Table 4 shows the yeast strains used in this study to study the effects of FLO11 on cell integrity. These strains were kindly provided by Todd Reynolds Ph.D. TBR1 is wild type expressing regular levels of FLO11, TBR4 is hyper adhesive strain which upregulates *flo11*; TBR5 is the *flo11* knockout strain that does not express protein. L6906 has a human influenza hemagglutinin (HA) epitope tag, used for the immuno gold labelling. L6906 carries a triple HA tag in the N-terminus of the FLO11 protein (Reynolds, Jansen et al. 2008). It has been reported that the HA tag does not affect flo11p protein function (Kraushaar, Bruckner et al. 2015).

Table 4. *S. Cerevisiae* Model Organisms with the different expressions of FLO11p. The gene modifications were provided by Todd Reynolds Lab.

Yeast	Description	Gene modification	Reference
TBR1	Wild type	MAT ura3–52 leu2::hisG his3::hisG	(Reynolds and Fink 2001)
TBR4-	(hyper-adhesive)	MAT2 sf11:1 Kan Mx6ura 30 his 30 leu 20	
TRB5	Flo11 knockout	MAT ura3–52 leu2::hisG his3::hisG flo11::kanMX	(Reynolds and Fink 2001)
L6906	Flo11 with tag	MATα ura3–52 his3::hisG FLO11::HA	(Reynolds, Jansen et al. 2008)

Rationale

Is the cell wall compromised by the interaction with the nanopillars found in the cicada wing? We compared adhesion for the cicada wing from strains of yeast with various levels of expression of the FLO11p. This is exemplified in Figure 21, where the difference in flocculation levels of the yeast strains becomes apparent 30 minutes after the yeast solutions where vortexed.

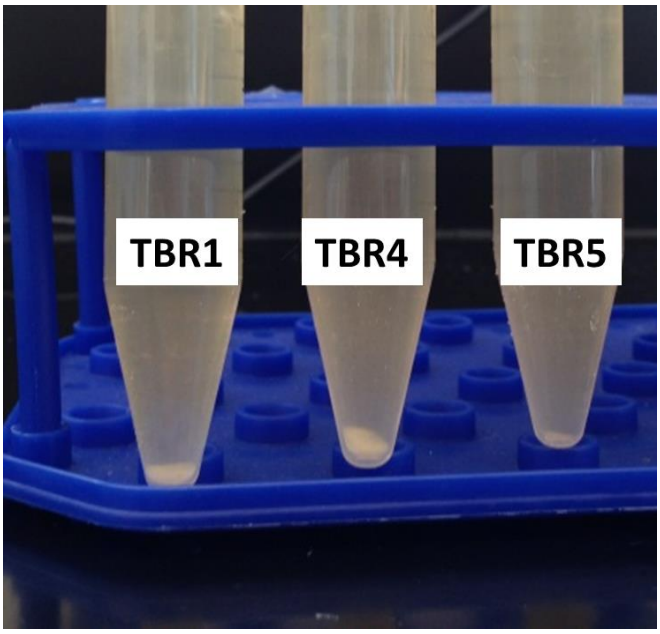

Figure 21. Flocculation of the Different Yeast Strains 30 minutes after vortex

Methods

One colony of each strain was immersed into 10 mL of YPD medium and grown overnight at 30·C 24 h incubation. Proceeded to transfer 1 ml of yeast solution and diluted it with 10 mL of YPD medium into a conical 15 mL centrifuge tube. Each tube had a cut of the outer cicada wing, which floated throughout the incubation and shaking period. The caps of the centrifuge tubes were left loose to release pressure from CO_2.

Yeast strains

TBR1, TBR4, TBR5, L6096

Our Objective was to use the SEM for the comparison of adhesion of the different yeast strains over a cicada wing.

Confocal adhesion experiment

Confocal microscopy remains as one of highest throughput techniques to evaluate microbe-surface dynamics. Though light microscopy has lower magnification and resolution when compared to electron and ion scanning microscopes, light microscopes do not require the extensive dehydration, fixation and coating like scanning beam microscopes do.

To set up a baseline we want to evaluate the adhesion dynamics of different strains of *S. cerevisiae* to a flat surface at different time points, to later be compared to the adhesion to surfaces with different nano-reliefs. Labelling of the cells will be done with calcofluor white, which binds to chitin (This might be problematic later when using the wings of the insect which are rich in chitin).

Results

To determine the incubation time needed for cells to be in early log phase of their growth we performed growth curves of the different yeast strains. The growth curves of the different strains can be seen in Figure 22. This growth curves show flocculation at the 20^{th} hour reading, and a general inflection in the growth after two hours. This allowed us to adjust our seeding parameter to the yeast procedure.

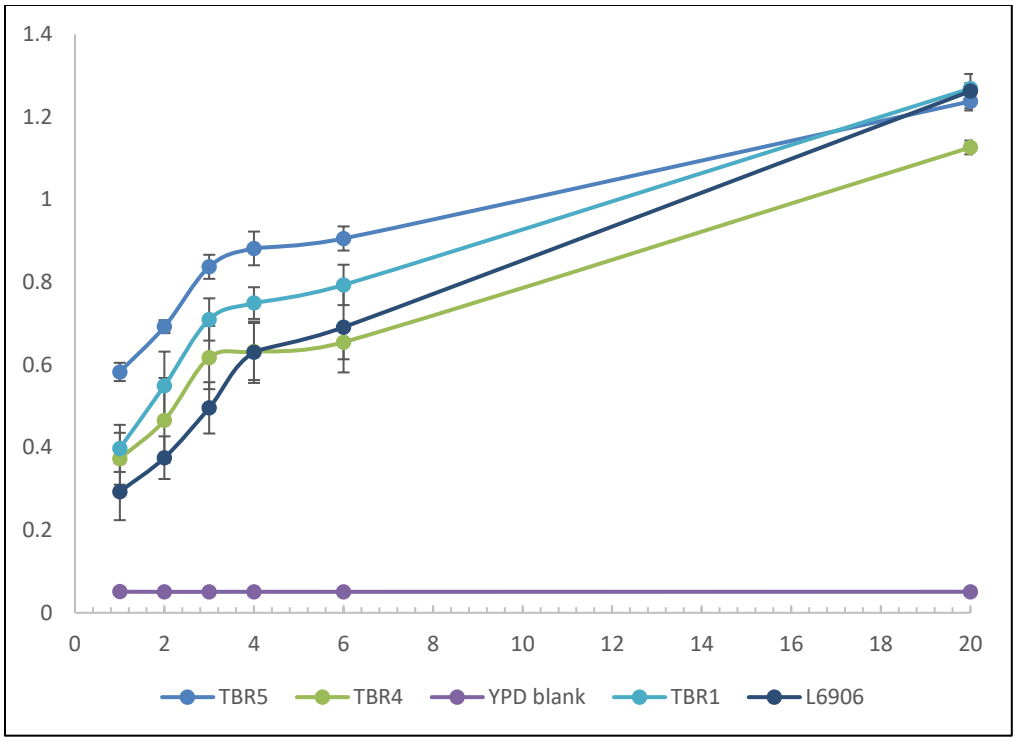

Figure 22. Growth Curves of the Yeast strains used among the different experiments throughout the document.

We performed a confocal analysis of yeast being deposited onto glass coverslips for 2 hours and found no significant difference among the different strains of TBR1, TBR4 and TBR5. As expected there was a significance difference among the diluted and undiluted samples of yeast but no difference among the groups themselves (see Figure 23). This finding dissuades us from using confocal microscopy for surface analysis, in addition that it would not be suited for surfaces with no or little optical transmittance.

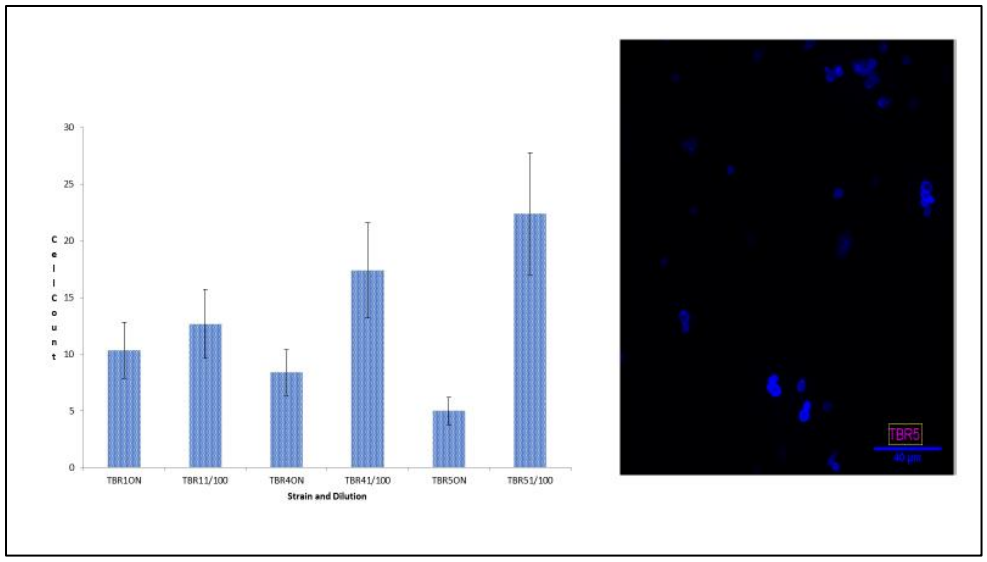

Figure 23. Confocal Study of the Yeast adhered to a Glass Slide. No significant difference was detected among the different strains. Typical micrograph of this study.

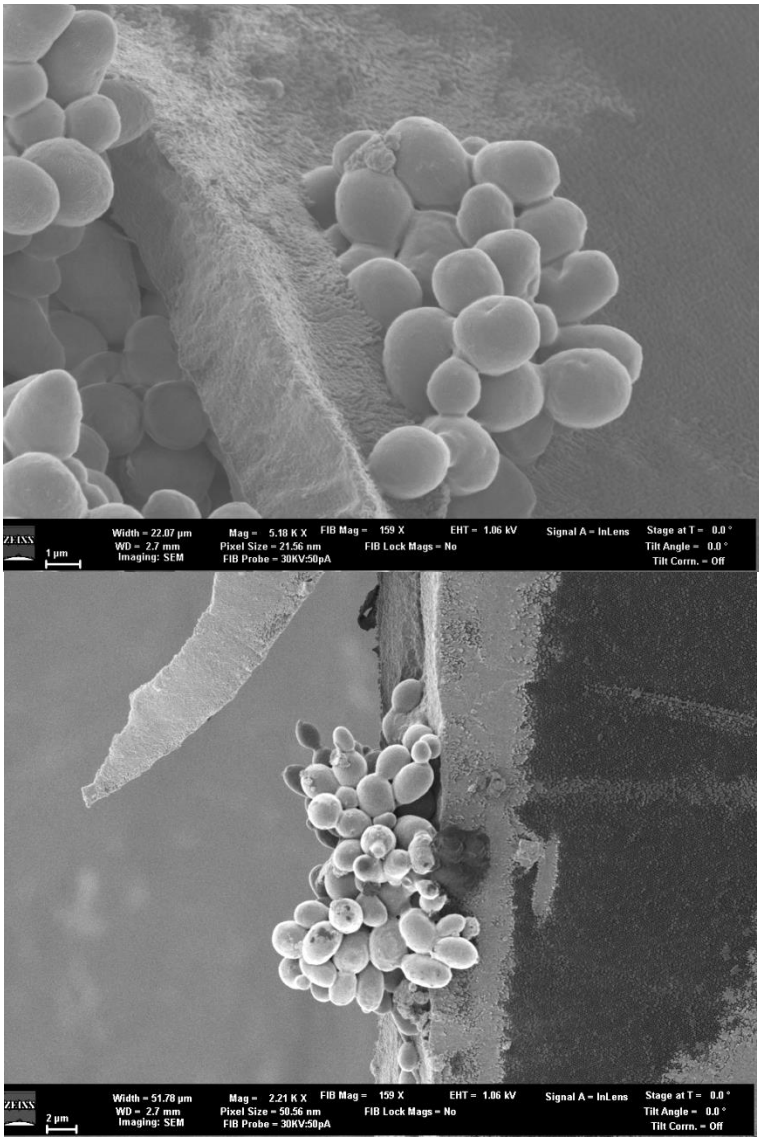

Figure 24. TBR1 Buds Adhered to the Edge of the Cicada Wing which was cut and does not present the roughness of as in the main wing. The author found that TBR1 had a preferential proliferation at the edge of the cicada wing.

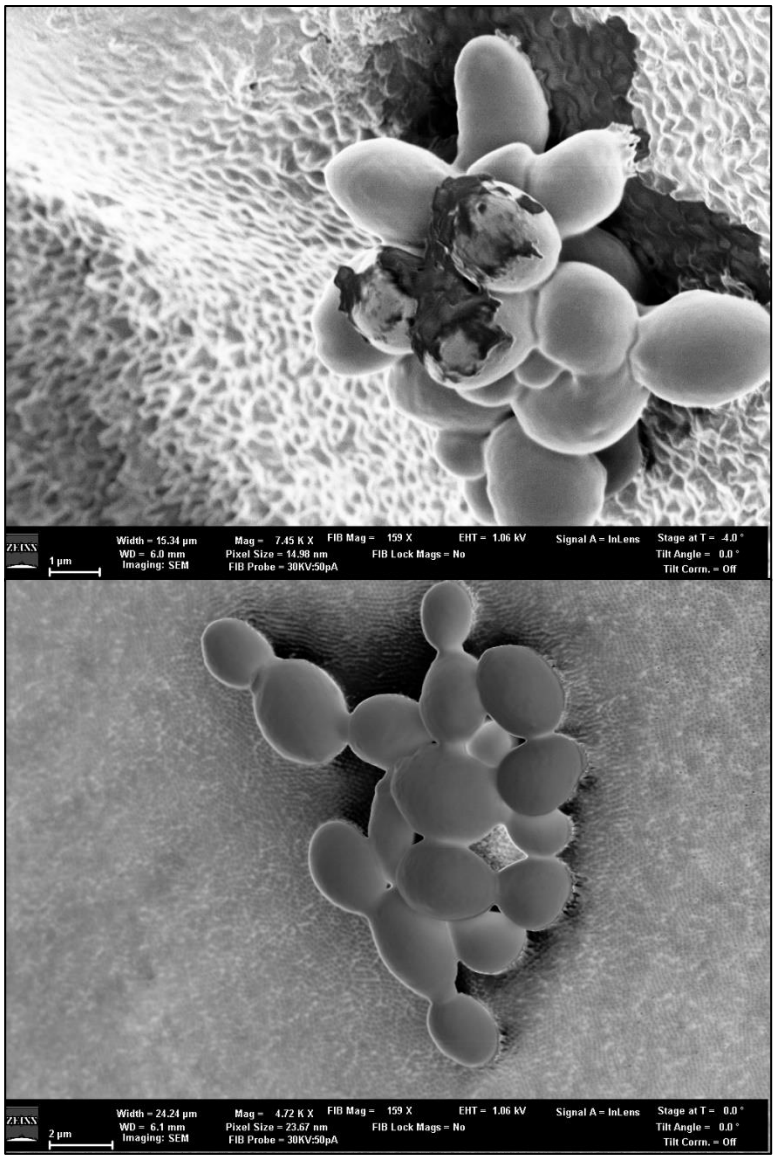

Figure 25. This is representative of the Micrograph of TBR4 Adhering to the Cicada Wing bed of Nanonails. A bit of a surprise as we expected a linear deleterious response to the expression of FLO11p interacting with the bed of nails. SEM SE image, FOV 15.34 µm.

Figure 26. Representative SEM Micrograph for the Cicada Wing exposed to TBR5. Yeast did not adhere to the cicada wing.

Using scanning probe microscopes, we demonstrated that the nanopillars found in the cicada wing provoked a significant deleterious effect on the TBR1 cells trying to adhere to the surface of the Cicada wing, while the TBR4 could adapt to the surface based on the hyperexpression of the FLO11p. While the knockout FLO11 strain of TBR5 had little adhesion to the surface, as it would be expected yet once adhere the NSS would perforate the cell membrane. We went to the extent of testing randomization procedure for the TBR5 lack of adhesion that we performed a composite image on one sample only to find one bud of yeast near the vein of the wing which has reduced nanopillar structures.

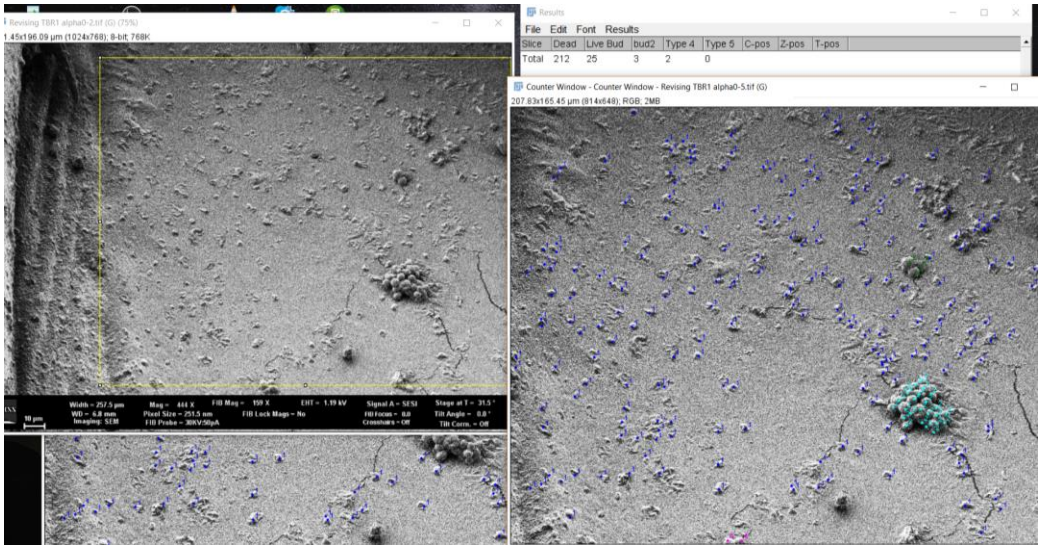

Figure 27. Shows TBR1 attached to a Cicada Wing Surface. SEM micrograph, SE/EHT detection, with a 10-nm carbon conductive coating.

Figure 27 illustrates the cell counting procedure using FIJI to quantify the number of compromised cells and intact cells on the surface. A region of interest of $3.44x10^{-1}$ mm^2 was selected to exclude the vein of the wing which resulted in 212 identified cells of compromised structure, with 30 cells still alive. It is worth noting that of the live cells, 25 were from a single bud. While the cells compromised were individual cells. The larger bud may have already agglomerated prior to the attachment to the cell surface, as the incubation was of 2 hours.

This shows that the hope of creating an antimicrobial surface solely based on geometry is not feasible approach, as surfaces like will eventually foul, and microbes that count with defensive mechanisms like that of hyper expression of adhesins will proliferate in these environments.

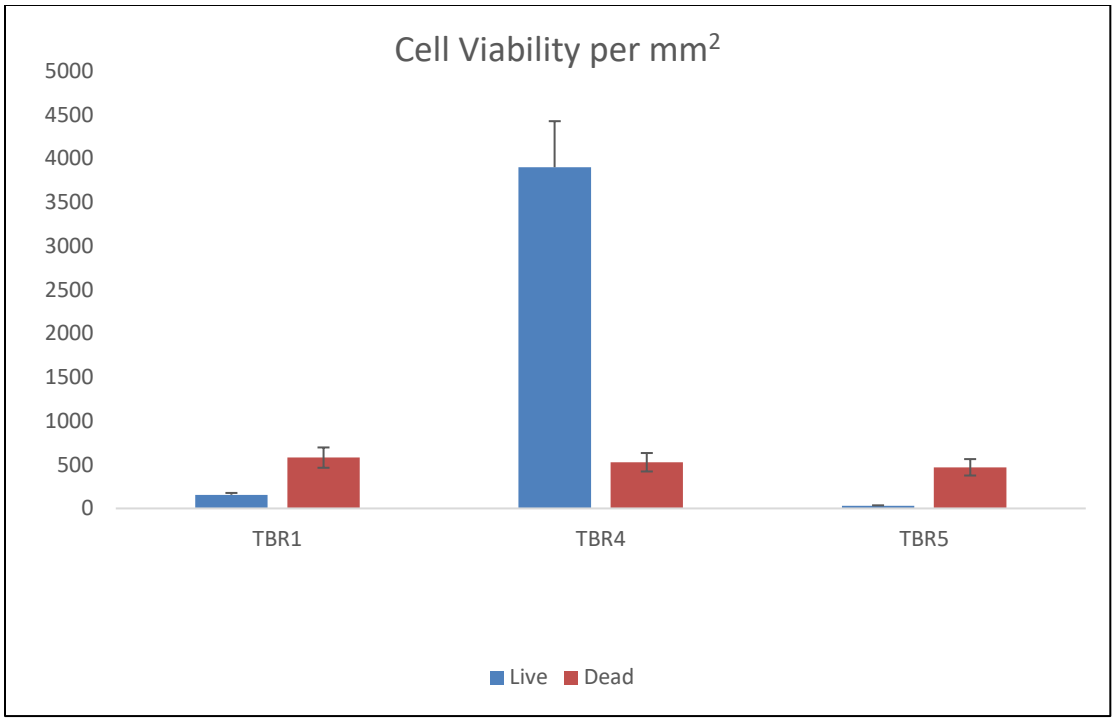

Figure 28. Response of the Different Strains to CW. The numbers represent are averaged over area of 1 mm^2.

Nanostructured Surface Induced Failure of *S. Cerevisiae* Cell Wall

Background

Rough surfaces like those found in the cicada and the dragonfly wing reduce the viability of bacteria and yeast. These nanostructured surfaces compromise the cell wall integrity of microorganism try to adhere to the surface. The NSS do not induce a toxic response on microbes like an antimycotic would on a yeast or an antibiotic on bacteria. Several theoretical models propose that the toxic effect is mechanistic result, in this study we examine the nanostructured penetration into the cell wall. Using high resolution Scanning Electron Microscope (SEM) and Helium Ion Microscope (HIM) we zoom into the contact point between the yeast and the surface of interest. We investigated whether

the nanopillars are in fact piercing the cell wall or is a result of rupturing stress from the cell overextending to adhere to a surface. We also compared the dimensions of the nanopillars within the same cicada wing.

Methods and Experimental Design

Yeast strains TBR1, TBR4 and TBR5 (see Table 4. *S. Cerevisiae* Model Organisms with the different expressions of FLO11p. The gene modifications were provided by Todd Reynolds Lab. The yeast was exposed to the surface during the early log phase. The early log phase presents the initial stages of adhesion and reduces flocs of yeast that may precipitates onto the surface of interest. After an overnight exposure the cicada wings were removed from the yeast growth media for EM sample preparation. The samples were fixed, dehydrated and sputtered with a 8 nm gold-palladium coat. Micrographs were collected following randomization, with an n=10. Once adhere yeast were identified from a 100 µm, we zoomed into the sample to measure the contact points between the yeast and the surface. We measured the length of suspected proteins and the nanopillars. We examined both sides of the cicada wing, to check that the effect was the same for both sides of the wing.

Results and Discussion

Comparison of both sides of the wing

We found that different sides of the same cicada wing, have significantly different dimensions. Measuring the tip of the nanopillar we found that Side 1 (S1) had a circular area of $(3.04 \pm 0.68) \times 10^3$ nm^2, in comparison flipping the wing, the tip of the nanopillar area measured $(1.14 \pm 0.18) \times 10^4$ nm^2. Both using the principle of two standard

deviations difference, and single factor ANNOVA (P<<0.01) we found a significant difference between the dimensions of the nanopillars. This is exemplified in Figure 29, by comparing both sides of the same wing micrographs and graphed.

To the best of our knowledge, the dimensions of the nanopillars in the same cicada wing have been treated as homogenous in the literature. Our lab has previously found that there are variations in nanopillar dimensions among distinct species. Yet this is the first time reported that there are significant variations within the sides of the same wing section. We recommend that this should be further investigated, with multiple surface characterization techniques. Additionally, we recommend that the dimensions of the nanopillars directly interacting with microorganisms be recorded when studying the antimicrobial properties of a wing.

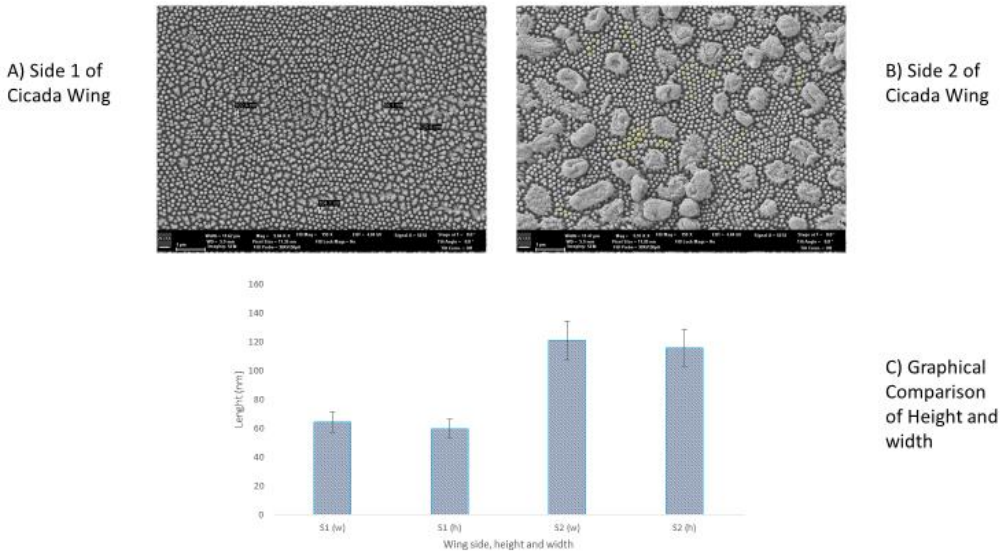

Figure 29. Representative Morphometric Measurements of Two Sides of the Cicada Wing. There was a difference in the dimensions of the nanopillars. B) Side two had

larger tips of nanopillars. C) Bar graph comparison of the nanopillars. n=38, error bar=Standard deviation.

Yeast Imprints

After assessing the nanopillars of both sides of sides of the wings, we had an unexpected result. While flipping the wing from the adhesive surface, yeast became unattached from the wing and exposed the plane of the yeast which adheres to the cicada wing surface. This plane shows a pattern of the nanopillars imprinted onto the wing. This allowed to see an inverted view where the yeast comes in contact point with the surface. This serendipitous find enabled us to observe something we had been previously unable to, and for future work this inversion should be explored.

The results of measuring pores on the cells were: the average circular area was $(1.67 \pm 0.68) \times 10^3$ nm^2, the average width was 46.5 ± 1.4 nm, and an average height of 52.1 ± 1.8 nm. These dimensions are within the range of the nanopillar dimensions. It should be noted that the pores are in fact larger as they were not adjusted for the addition of 8 nm conductive coating.

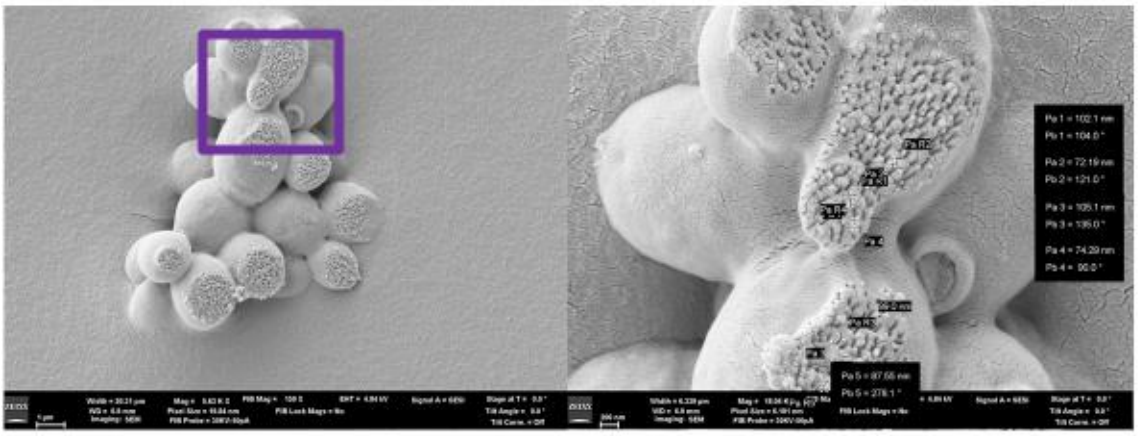

Figure 30. TBR4 Cells, right image is a magnification of the left micrograph. Shows the penetration of the nanopillars on TBR4. These cells were the least compromised by NSS, and this can be seen by flipping the cells that the nanopillars do not penetrate the cell wall. These micrographs were taken with the SEM SE detector, samples had a conductive coating 14 nm thick Au/Pt. Scalebar of left image=1 µm, while the right scale bar =2 nm.

CHAPTER V

CONCLUSIONS

This works used high magnification scanning particle beam microscopy to evaluate to zoom into the adhesion contact points between a surface and a microorganism. We examined different expressions of FLO11p in the adhesion and interaction of yeast with nanostructured surfaces. FLO11p is a well-studied and characterized protein, making it a suitable subject for high resolution protein localization. We showed the proteins interacting with different substrates in the preliminary stages of adhesion. Mitigating adhesion is critical for control of biofilm formation. The work presented throughout this document brings the study of microorganisms from the micron scale to the nanometer scale in a three-dimensional manner.

Throughout this work we further confirm the importance of length of the adhesion protein for cell survivability. We pinpointed the location of the within the cell and the surface. FLO11p is usually found around the bud scars of the yeast and the lateral axial positions, which helped it adhere to different surfaces and other cells forming buds.

We saw that cell agglomerations helped the yeast withstand the effects of the NSS surfaces, while individual cells that encountered the NSS tended to end up in cell disruption. Higher expression of FLO11p allowed the yeast to cover the Nanopillars with ECM, avoiding perforation from the nanopillar. This is useful as adhesion has not been taking into consideration when modelling the interaction between microbes and NSS.

We used a yeast expressing various levels of FLO11p to test the protein relationship with adhesion and survival of the yeast. Despite that we saw differences in the micrographs among the strains. We had to confirm that these differences were not an effect of artifacts. This drove us to use immuno gold labelling for the SEM. We improved on the immunogold labelling techniques by encouraging the use of the EDS detector. We developed a technique to use EDS for immunogold of 20 nm labelling a whole cell on a substrate in a three-dimensional manner.

We demonstrated that by using SEM-EDS we are able confirm the presence and location of the immunogold label in a three-dimensional micrograph. This work is unique as EDS is generally not used at the magnification necessary to resolve the adhesion between a microbial cell and a surface. We recommend using EDS to overcome any potential artifacts that may arise from using SE/BSE stacking or SE morphometrical measurements as standalone techniques.

With the SEM-EDS detection and the HIM, we detected the immunogold on samples without a conductive coating. Though this endeavor was non-trivial, as several parameters must be adjusted by the microscopist when sampling, making it unsuitable as a streamline process. To improve the signal using the HIM for uncoated samples, we used the Flood gun and a metallic substrate to increase the contrast on the uncoated sample. The SEM was unable to detect the immunogold label on uncoated samples with the SE detector. When examining the uncoated samples with the SEM SE detector, the samples had excessive charging even at low beam voltages. Using BSE detector, we

could pinpoint the location but charging was still a major factor interfering with the image.

With the Helium Ion Microscope, we demonstrated that it is possible to locate a 20 nm immunogold with a thin carbon layer on the cells in whole cells using only an SE detector. This surpasses the SEM capabilities, which was limited to 30-40 nm probe size for immuno labels and SE detection. The HIM also presents a larger depth of field in its images allowing for a better perspective of the whole cell interaction.

The HIM Orion has a couple of drawbacks; within the design, the main chamber is large and works under ultra-high vacuum. This large chamber requires a lot of time to reach the pressure to the nanoTorr range needed for operation. In the HIM-Orion model, the loading chamber is also large, designed for enabling plasma cleaning of the sample. Yet, this as well requires extensive time in equilibrating from atmospheric pressure to the 100 nanoTorr pressure range needed to load into the chamber. This limits the potential of the HIM Orion to be used as a manufacturing tool. In a newer model, the Nanofab, the loading dock and the sample chamber are smaller in size increasing the throughput capabilities.

S. cerevisiae uses FLO11p as an adhesion protein to adhere to surfaces and other cells.(Douglas, Li et al. 2007) The process of cellular adhesion is a critical first step in the formation of Biofilms. For this reason, a better approach is needed to quantitatively evaluate the surface interaction that reduces the viability of microorganisms. To overcome these problems, we propose an innovative method to study the effect on viability of yeast cells in Aim I of this dissertation. Due to the small pseudo two-

dimensional scale of these surfaces, microscopy must be used in a quantitative matter to understand the reduction in cell viability. But, even high magnification light microscopes are unable to resolve the details of the nanopillar interaction (Kizilyaprak, Bittermann et al. 2014). For this reason, we relied on scanning beam and particle microscopes to study the interaction of these structures with the yeast.

In this dissertation we examine *S. cerevisiae* disruption of cell wall integrity when exposed to nanosurfaces, we suspect that the adhesin/floculin glyco protein located in the cell surface plays a critical role in this disruption. Cell adhesion can be understood as the extracellular binding between cell-cell or cell-surface.

For qualitative chemical confirmation of the presence of FLO11p in a sample of interest, we presented an immunogold labelling technique ratified via SEM+EDS, while high magnification analysis was done with the HIM. Our method expands the use of electron microscopy by coupling the technique with immuno-gold chemistry and chemically identifying the nanoparticle using Energy Dispersive X-ray Spectroscopy (EDS). We localized the proteins within the scale of the nanopillars, and we determined that FLO11 is the adhesion protein, which *S. cerevisiae* uses to adhere to surfaces. The nano-topographies compromised the integrity of yeast cell wall of *S. cerevisiae* not in the linear fashion as we had expected. As previously discussed, the dynamics of these cell disruptions are not well understood, and I showed that adhesion proteins (adhesins) do have an effect in these dynamics. To label the proteins, we used 20 nm gold nanoparticles (AuNP) conjugated with secondary antibody bounded to a primary

antibody bound to a genetically inserted HA-epitope tag found at the C-terminal of protein Flo 11 in the L6906 strain.

We have found that modifying the tilt angle improves the signal of our gold label. We have also seen that optimizing the scattering by limiting interference from the sample in its path to the detector show the importance of minimizing the interference of other elements when trying to localize the gold label. We present a practical guide to pinpoint proteins on whole cells in a three-dimensional manner and use FLO11p as our controlled study subject.

This work was ultimately to uncover the invisible. Like the blind person of the parable, I look under and above the microscopic elephant through multiple minute images to get the big picture.

REFERENCES

- Adams, R. M. and Smithm George W. (1977). "An S.E.M. Survey of the Five Carnivorous Pitcher Plant Genera." American Journal of Botany **64**(3): 265-272.
- Alkilany, A., R. Frey, J. Ferry and C. Murphy (2008). "Gold Nanorods as Nanoadmicelles: 1-Naphthol Partitioning into a Nanorod-Bound Surfactant Bilayer."
- Baer, D. R., M. H. Engelhard, G. E. Johnson, J. Laskin, J. Lai, K. Mueller, P. Munusamy, S. Thevuthasan, H. Wang, N. Washton, A. Elder, B. L. Baisch, A. Karakoti, S. V. N. T. Kuchibhatla and D. Moon (2013). "Surface characterization of nanomaterials and nanoparticles: Important needs and challenging opportunities." Journal of Vacuum Science and Technology A: Vacuum, Surfaces and Films **31**(5).
- Bandara, C. D., S. Singh, I. O. Afara, A. Wolff, T. Tesfamichael, K. Ostrikov and A. Oloyede (2017). "Bactericidal Effects of Natural Nanotopography of Dragonfly Wing on Escherichia coli." ACS Appl Mater Interfaces **9**(8): 6746-6760.
- Bell, D. C. (2009). "Contrast mechanisms and image formation in helium ion microscopy." Microsc Microanal **15**(2): 147-153.
- Betzig, E., G. H. Patterson, R. Sougrat, O. W. Lindwasser, S. Olenych, J. S. Bonifacino, M. W. Davidson, J. Lippincott-Schwartz and H. F. Hess (2006). "Imaging Intracellular Fluorescent Proteins at Nanometer Resolution." Science **313**(5793): 1642-1645.
- Bhushan, B. and Y. Chae Jung (2007). "Wetting study of patterned surfaces for superhydrophobicity." Ultramicroscopy **107**(10-11): 1033-1041.
- Blevins, S. M. and M. S. Bronze (2010). "Robert Koch and the 'golden age' of bacteriology." International Journal of Infectious Diseases **14**(9): e744-e751.
- Bolte, S. and F. P. Cordelieres (2006). "A guided tour into subcellular colocalization analysis in light microscopy." Journal of Microscopy **224**(3): 213-232.
- Bormashenko, E., Y. Bormashenko, T. Stein, G. Whyman and E. Bormashenko (2007). "Why do pigeon feathers repel water? Hydrophobicity of pennae, Cassie–Baxter wetting hypothesis and Cassie–Wenzel capillarity-induced wetting transition." Journal of Colloid and Interface Science **311**(1): 212-216.
- Bou Zeidan, M., L. Carmona, S. Zara and J. F. Marcos (2013). "FLO11 Gene Is Involved in the Interaction of Flor Strains of Saccharomyces cerevisiae with a Biofilm-Promoting Synthetic Hexapeptide." Appl Environ Microbiol **79**(19): 6023-6032.
- Bou Zeidan, M., G. Zara, C. Viti, F. Decorosi, I. Mannazzu, M. Budroni, L. Giovannetti and S. Zara (2014). "L-Histidine Inhibits Biofilm Formation and FLO11-Associated Phenotypes in Saccharomyces cerevisiae Flor Yeasts." PLoS One **9**(11): e112141.

- Bowen, W. R., R. W. Lovitt and C. J. Wright (2001). "Atomic Force Microscopy Study of the Adhesion of Saccharomyces cerevisiae." Journal of Colloid and Interface Science **237**(1): 54-61.
- Boyde, A. and C. Wood (1969). "Preparation of animal tissues for surface-scanning electron microscopy." Journal of Microscopy **90**(3): 221-249.
- Boyoglu, C., Q. He, G. Willing, S. Boyoglu-Barnum, V. A. Dennis, S. Pillai and S. R. Singh (2013). "Microscopic Studies of Various Sizes of Gold Nanoparticles and Their Cellular Localizations." ISRN Nanotechnology **2013**: 1-13.
- Braus, G. H., O. Grundmann, S. Brückner and H.-U. Mösch (2003). "Amino Acid Starvation and Gcn4p Regulate Adhesive Growth and FLO11 Gene Expression in Saccharomyces cerevisiae." Molecular Biology of the Cell **14**(10): 4272-4284.
- Breuer, G. (1984). "A Formal Representation of Abbe's Theory of Microscopic Image Formation." Optica Acta: International Journal of Optics **31**(6): 661-670.
- Bruckner, S. and H. U. Mosch (2012). "Choosing the right lifestyle: adhesion and development in Saccharomyces cerevisiae." FEMS Microbiol Rev **36**(1): 25-58.
- Cassie, A. B. D. and S. Baxter (1944). "Wettability of porous surfaces." Transactions of the Faraday Society **40**(0): 546-551.
- Castro-Longoria, E., A. R. Vilchis-Nestor and M. Avalos-Borja (2011). "Biosynthesis of silver, gold and bimetallic nanoparticles using the filamentous fungus Neurospora crassa." Colloids Surf B Biointerfaces **83**(1): 42-48.
- Chandra, J., D. M. Kuhn, P. K. Mukherjee, L. L. Hoyer, T. McCormick and M. A. Ghannoum (2001). "Biofilm Formation by the Fungal Pathogen Candida albicans: Development, Architecture, and Drug Resistance." Journal of Bacteriology **183**(18): 5385-5394.
- Chen, C. and J. Wang (2008). "Investigating the interaction mechanism between zinc and Saccharomyces cerevisiae using combined SEM-EDX and XAFS." Appl Microbiol Biotechnol **79**(2): 293-299.
- Claude, A., K. R. Porter and E. G. Pickels (1947). "Electron microscope study of chicken tumor cells." Cancer Research **7**(7): 421-430.
- Costerton, J. W., K. J. Cheng, G. G. Geesey, T. I. Ladd, J. C. Nickel, M. Dasgupta and T. J. Marrie (1987). "Bacterial biofilms in nature and disease." Annu Rev Microbiol **41**: 435-464.
- de Jonge, N., R. Sougrat, B. M. Northan and S. J. Pennycook (2010). "Three-dimensional scanning transmission electron microscopy of biological specimens." Microsc Microanal **16**(1): 54-63.
- De Kruif, P. (1996). Microbe hunters, Houghton Mifflin Harcourt.
- Dellieu, L., M. Sarrazin, P. Simonis, O. Deparis and J. P. Vigneron (2014). "A two-in-one superhydrophobic and anti-reflective nanodevice in the grey cicada Cicada orni (Hemiptera)." Journal of Applied Physics **116**(2): 024701.
- Dhillon, G. S., S. Kaur, S. K. Brar and M. Verma (2012). "Flocculation and Haze Removal from Crude Beer Using In-House Produced Laccase from Trametes

versicolor Cultured on Brewer's Spent Grain." Journal of Agricultural and Food Chemistry **60**(32): 7895-7904.
- Douglas, L. M., L. Li, Y. Yang and A. M. Dranginis (2007). "Expression and characterization of the flocculin Flo11/Muc1, a Saccharomyces cerevisiae mannoprotein with homotypic properties of adhesion." Eukaryot Cell **6**(12): 2214-2221.
- Drummond, S. P. and T. D. Allen (2008). "From live-cell imaging to scanning electron microscopy (SEM): the use of green fluorescent protein (GFP) as a common label." Methods in cell biology **88**: 97-108.
- Echlin, P. (2009). "Handbook of Sample Preparation for Scanning Electron Microscopy and X-Ray Microanalysis-Springer US."
- Faulk, W. P. and G. M. Taylor (1971). "An immunocolloid method for the electron microscope." Immunochemistry **8**(11): 1081-1083.
- Fitzgerald, R., K. Keil and F. J. H. Kurt (1968). "Solid-State Energy-Dispersion Spectrometer for Electron-Microprobe X-ray Analysis." Science **159**(3814): 528-530.
- Fleet, G. (2003). "Yeast interactions and wine flavour." International Journal of Food Microbiology **86**(1-2): 11-22.
- Fleet, G. H. (2003). "Yeast interactions and wine flavour." International Journal of Food Microbiology **86**(1–2): 11-22.
- Fu, G., T. Huang, J. Buss, C. Coltharp, Z. Hensel and J. Xiao (2010). "In vivo structure of the E. coli FtsZ-ring revealed by photoactivated localization microscopy (PALM)." PloS one **5**(9): e12680.
- Fürstner, R., W. Barthlott, C. Neinhuis and P. Walzel (2005). "Wetting and Self-Cleaning Properties of Artificial Superhydrophobic Surfaces." Langmuir **21**(3): 956-961.
- Gest, H. (2004). "The Discovery of Microorganisms by Robert Hooke and Antoni van Leeuwenhoek, Fellows of the Royal Society." Notes and Records of the Royal Society of London **58**(2): 187-201.
- Giannuzzi, L. A. and F. A. Stevie (1999). "A review of focused ion beam milling techniques for TEM specimen preparation." Micron **30**(3): 197-204.
- Glinel, K., P. Thebault, V. Humblot, C. M. Pradier and T. Jouenne (2012). "Antibacterial surfaces developed from bio-inspired approaches." Acta Biomater **8**(5): 1670-1684.
- GmbH, B. N. (© 2011 Bruker Nano GmbH, Berlin, Germany). "Introduction to EDS analysis-Reference Manual."
- Goldberg, M. W. and J. Fiserova (2016). "Immunogold Labeling for Scanning Electron Microscopy." Methods Mol Biol **1474**: 309-325.
- Goldstein, J., D. E. Newbury, P. Echlin, D. C. Joy, A. D. Romig Jr, C. E. Lyman, C. Fiori and E. Lifshin (2012). Scanning electron microscopy and X-ray microanalysis: a text for biologists, materials scientists, and geologists, Springer Science & Business Media.

- Goossens, K. V., F. S. Ielasi, I. Nookaew, I. Stals, L. Alonso-Sarduy, L. Daenen, S. E. Van Mulders, C. Stassen, R. G. van Eijsden, V. Siewers, F. R. Delvaux, S. Kasas, J. Nielsen, B. Devreese and R. G. Willaert (2015). "Molecular mechanism of flocculation self-recognition in yeast and its role in mating and survival." MBio **6**(2).
- Gosline, J. M., P. A. Guerette, C. S. Ortlepp and K. N. Savage (1999). "The mechanical design of spider silks: from fibroin sequence to mechanical function." Journal of Experimental Biology **202**(23): 3295.
- Gounon, P. and C. Le Bouguenec (1999). "Immunogold-labelling in Scanning Electron Microscopy-Detection of adhesins at the surface of Pathogenic Escherichia Coli strains." JEOL News **34E**(No.1): 4.
- Gregor Hlawacek, V. V., Raoul van Gastel, Bene Poelsema (2014). "Helium Ion microscopy." Physics of Interfaces and Nanomaterials, MESA.
- Guo Bing, Styles Cora A., Feng Qinghua and Fink Gerald R (2000). "A Saccharomyces gene family involved in invasive growth, cell–cell adhesion, and mating." Proceedings of the National Academy of Sciences **97**(22): 12158-12163.
- Gustafsson, M. G. L. (2001). "Surpassing the lateral resolution limit by a factor of two using structured illumination microscopy." Journal of Microscopy **198**(2): 82-87.
- Hall, A. R. (2013). "In situ thickness assessment during ion milling of a free-standing membrane using transmission helium ion microscopy." Microsc Microanal **19**(3): 740-744.
- Halme, A., S. Bumgarner, C. Styles and G. R. Fink (2004). "Genetic and Epigenetic Regulation of the FLO Gene Family Generates Cell-Surface Variation in Yeast." Cell **116**(3): 405-415.
- Harutyunyan, H., S. Palomba, J. Renger, R. Quidant and L. Novotny (2010). "Nonlinear dark-field microscopy." Nano Lett **10**(12): 5076-5079.
- Hasan, J., R. J. Crawford and E. P. Ivanova (2013). "Antibacterial surfaces: the quest for a new generation of biomaterials." Trends in Biotechnology **31**(5): 295-304.
- Hasan, J., H. K. Webb, V. K. Truong, S. Pogodin, V. A. Baulin, G. S. Watson, J. A. Watson, R. J. Crawford and E. P. Ivanova (2013). "Selective bactericidal activity of nanopatterned superhydrophobic cicada Psaltoda claripennis wing surfaces." Appl Microbiol Biotechnol **97**(20): 9257-9262.
- Hermann, R., P. Walther and M. Müller (1996). "Immunogold labeling in scanning electron microscopy." Histochemistry and Cell Biology **106**(1): 31-39.
- Hobley, L., C. Harkins, C. E. MacPhee and N. R. Stanley-Wall (2015). "Giving structure to the biofilm matrix: an overview of individual strategies and emerging common themes." FEMS Microbiol Rev **39**(5): 649-669.
- Hodges, G. M., J. Southgate and E. C. Toulson (1987). "Colloidal gold--a powerful tool in scanning electron microscope immunocytochemistry: an overview of bioapplications." Scanning microscopy **1**(1): 301-318.
- Hohmann, S. (2002). "Osmotic Stress Signaling and Osmoadaptation in Yeasts." Microbiology and Molecular Biology Reviews **66**(2): 300-372.

- Hooke, R. (1664). Micrographia: or some physiological descriptions of minute bodies made by magnifying glasses, with observations and inquiries thereupon, Courier Corporation.
- Hori, K. and S. Matsumoto (2010). "Bacterial adhesion: From mechanism to control." Biochemical Engineering Journal **48**(3): 424-434.
- Horisberger, M., J. Rosset and H. Bauer (1975). "Colloidal gold granules as markers for cell surface receptors in the scanning electron microscope." Experientia **31**(10): 1147-1149.
- Hoyer, L. C., J. C. Lee and C. Bucana (1979). "Scanning immunoelectron microscopy for the identification and mapping of two or more antigens on cell surfaces." Scanning electron microscopy(3): 629-636.
- Hu, M., C. Novo, A. Funston, H. Wang, H. Staleva, S. Zou, P. Mulvaney, Y. Xia and G. V. Hartland (2008). "Dark-field microscopy studies of single metal nanoparticles: understanding the factors that influence the linewidth of the localized surface plasmon resonance." Journal of materials chemistry **18**(17): 1949-1960.
- Ivanova, E. P., J. Hasan, H. K. Webb, G. Gervinskas, S. Juodkazis, V. K. Truong, A. H. Wu, R. N. Lamb, V. A. Baulin, G. S. Watson, J. A. Watson, D. E. Mainwaring and R. J. Crawford (2013). "Bactericidal activity of black silicon." Nat Commun **4**: 2838.
- Ivanova, E. P., J. Hasan, H. K. Webb, V. K. Truong, G. S. Watson, J. A. Watson, V. A. Baulin, S. Pogodin, J. Y. Wang, M. J. Tobin, C. Löbbe and R. J. Crawford (2012). "Natural Bactericidal Surfaces: Mechanical Rupture of Pseudomonas aeruginosa Cells by Cicada Wings." Small **8**(16): 2489-2494.
- J. De Mey, M. M., G. Geuens. R. Nuydens and M. De Brabander (1981). "Mey et all 1981 High resoultion Light and Electron microscopic localization of tubulin with IGS (immuno gold staining) method.pdf." Cell Biology International Reports **5**(9): 889-900.
- Jayabalan, R., K. Malini, M. Sathishkumar, K. Swaminathan and S.-E. Yun (2010). "Biochemical characteristics of tea fungus produced during kombucha fermentation." Food Science and Biotechnology **19**(3): 843-847.
- Kalhor, N., S. A. Boden and H. Mizuta (2014). "Sub-10nm patterning by focused He-ion beam milling for fabrication of downscaled graphene nano devices." Microelectronic Engineering **114**: 70-77.
- Kanaya, K. and H. Kawakatsu (1972). "Secondary electron emission due to primary and backscattered electrons." Journal of Physics D: Applied Physics **5**(9): 1727.
- Karunanithi, S., N. Vadaie, C. A. Chavel, B. Birkaya, J. Joshi, L. Grell and P. J. Cullen (2010). "Shedding of the mucin-like flocculin Flo11p reveals a new aspect of fungal adhesion regulation." Curr Biol **20**(15): 1389-1395.
- Kempen, P. J., C. Hitzman, L. S. Sasportas, S. S. Gambhir and R. Sinclair (2013). Advanced characterization techniques for nanoparticles for cancer research: Applications of SEM and NanoSIMS for locating au nanoparticles in cells. Materials Research Society Symposium Proceedings.

- Kempen, P. J., A. S. Thakor, C. Zavaleta, S. S. Gambhir and R. Sinclair (2013). "A scanning transmission electron microscopy approach to analyzing large volumes of tissue to detect nanoparticles." Microscopy and Microanalysis **19**(5): 1290-1297.
- Kim, K. Y., A. W. Truman, S. Caesar, G. Schlenstedt and D. E. Levin (2010). "Yeast Mpk1 cell wall integrity mitogen-activated protein kinase regulates nucleocytoplasmic shuttling of the Swi6 transcriptional regulator." Mol Biol Cell **21**(9): 1609-1619.
- Kiseleva, E., T. D. Allen, S. A. Rutherford, S. Murray, K. Morozova, F. Gardiner, M. W. Goldberg and S. P. Drummond (2007). "A protocol for isolation and visualization of yeast nuclei by scanning electron microscopy (SEM)." Nature protocols **2**(8): 1943-1953.
- Kizilyaprak, C., A. G. Bittermann, J. Daraspe and B. M. Humbel (2014). "FIB-SEM tomography in biology." Methods Mol Biol **1117**: 541-558.
- Klang, V., C. Valenta and N. B. Matsko (2013). "Electron microscopy of pharmaceutical systems." Micron **44**: 45-74.
- Kobayashi Osamu, Hayashi Nobuyuki, Kuroki Ryota and Sone Hidetaka (1998). "Region of Flo1 Proteins Responsible for Sugar Recognition." Journal of Bacteriology **180**(24): 6503-6510.
- Köhler, H. (1981). "On Abbe's theory of image formation in the microscope." Optica Acta: International Journal of Optics **28**(12): 1691-1701.
- Kraushaar, T., S. Bruckner, M. Veelders, D. Rhinow, F. Schreiner, R. Birke, A. Pagenstecher, H. U. Mosch and L. O. Essen (2015). "Interactions by the Fungal Flo11 Adhesin Depend on a Fibronectin Type III-like Adhesin Domain Girdled by Aromatic Bands." Structure **23**(6): 1005-1017.
- Kuisma-Kursula, P. (2000). "Accuracy, Precision and Detection Limits of SEM-WDS, SEM-EDS and PIXE in the Multi-Elemental Analysis of Medieval Glass." X-Ray Spectrometry **29**: 111-118.
- Levin, D. E. (2005). "Cell wall integrity signaling in Saccharomyces cerevisiae." Microbiol Mol Biol Rev **69**(2): 262-291.
- Levin, D. E. (2011). "Regulation of cell wall biogenesis in Saccharomyces cerevisiae: the cell wall integrity signaling pathway." Genetics **189**(4): 1145-1175.
- Li, X.-M., D. Reinhoudt and M. Crego-Calama (2007). "What do we need for a superhydrophobic surface? A review on the recent progress in the preparation of superhydrophobic surfaces." Chemical Society Reviews **36**(8): 1350-1368.
- Li, X. (2016). "Bactericidal mechanism of nanopatterned surfaces." Phys Chem Chem Phys **18**(2): 1311-1316.
- Li, X. M., D. Reinhoudt and M. Crego-Calama (2007). "What do we need for a superhydrophobic surface? A review on the recent progress in the preparation of superhydrophobic surfaces." Chem Soc Rev **36**(8): 1350-1368.
- Liu, T. L. and C.-J. C. Kim (2014). "Turning a surface superrepellent even to completely wetting liquids." Science **346**(6213): 1096-1100.

- Lloyd, G. E. and B. Freeman (1991). "SEM electron channelling analysis of dynamic recrystallization in a quartz grain." Journal of Structural Geology **13**(8): 945-953.
- Lo, W. S. and A. M. Dranginis (1998). "The cell surface flocculin Flo11 is required for pseudohyphae formation and invasion by Saccharomyces cerevisiae." Mol Biol Cell **9**(1): 161-171.
- Loukanov, A., N. Kamasawa, R. Danev, R. Shigemoto and K. Nagayama (2010). "Immunolocalization of multiple membrane proteins on a carbon replica with STEM and EDX." Ultramicroscopy **110**(4): 366-374.
- Lu, X., Z. Zhuang, Q. Peng and Y. Li (2011). "Wurtzite Cu2ZnSnS4 nanocrystals: a novel quaternary semiconductor." Chemical Communications **47**(11): 3141-3143.
- Lucas, M. S., M. Guenthert, P. Gasser, F. Lucas and R. Wepf (2014). "Correlative 3D imaging: CLSM and FIB-SEM tomography using high-pressure frozen, freeze-substituted biological samples." Methods Mol Biol **1117**: 593-616.
- Lui, C. H., L. Liu, K. F. Mak, G. W. Flynn and T. F. Heinz (2009). "Ultraflat graphene." Nature **462**(7271): 339-341.
- Masters, B. R. (2008). "History of the optical microscope in cell biology and medicine." eLS.
- Melngailis, J. (1993). "Focused ion beam lithography." Nuclear Instruments and Methods in Physics Research Section B: Beam Interactions with Materials and Atoms **80-81**: 1271-1280.
- Meyer, J. C., A. K. Geim, M. I. Katsnelson, K. S. Novoselov, T. J. Booth and S. Roth (2007). "The structure of suspended graphene sheets." Nature **446**: 60.
- Miki BL, Poon NH and Seligy VL (1982). "Repression and induction of flocculation interactions in Saccharomyces cerevisiae." J Bacteriol **150**(2): 880-889.
- Morikawa, J., M. Ryu, G. Seniutinas, A. Balcytis, K. Maximova, X. Wang, M. Zamengo, E. P. Ivanova and S. Juodkazis (2016). "Nanostructured Antireflective and Thermoisolative Cicada Wings." Langmuir **32**(18): 4698-4703.
- Murtey, M. D. (2016). Immunogold Techniques in Electron Microscopy. Modern Electron Microscopy in Physical and Life Sciences. M. Janecek and R. Kral. Rijeka, InTech**:** Ch. 07.
- Nanda, G., G. Hlawacek, S. Goswami, K. Watanabe, T. Taniguchi and P. F. A. Alkemade (2017). "Electronic transport in helium-ion-beam etched encapsulated graphene nanoribbons." Carbon **119**: 419-425.
- Newbury, D. E. and N. W. Ritchie (2013). "Is scanning electron microscopy/energy dispersive X-ray spectrometry (SEM/EDS) quantitative?" Scanning **35**(3): 141-168.
- Nobile, C. J. and A. P. Mitchell (2006). "Genetics and genomics of Candida albicans biofilm formation." Cell Microbiol **8**(9): 1382-1391.
- Notte, J. and B. Goetze (2014). "Imaging with the Helium Ion Microscope." 171-194.
- Nowlin, K., A. Boseman, A. Covell and D. LaJeunesse (2015). "Adhesion-dependent rupturing of Saccharomyces cerevisiae on biological antimicrobial nanostructured surfaces." J R Soc Interface **12**(102): 20140999.

- Orlov, I., A. Schertel, G. Zuber, B. Klaholz, R. Drillien, E. Weiss, P. Schultz and D. Spehner (2015). "Live cell immunogold labelling of RNA polymerase II." Scientific reports **5**: 8324-8324.
- Otto, K. (2008). "Biophysical approaches to study the dynamic process of bacterial adhesion." Res Microbiol **159**(6): 415-422.
- Owen, G. R., D. O. Meredith, I. Ap Gwynn and R. G. Richards (2001). "ENHANCEMENT OF IMMUNOGOLD-LABELLED FOCAL ADHESION SITES IN FIBROBLASTS CULTURED ON METAL SUBSTRATES: PROBLEMS AND SOLUTIONS." Cell Biology International **25**(12): 1251-1259.
- Pandey, P., M. S. Packiyaraj, H. Nigam, G. S. Agarwal, B. Singh and M. K. Patra (2014). "Antimicrobial properties of CuO nanorods and multi-armed nanoparticles against B. anthracis vegetative cells and endospores." Beilstein J Nanotechnol **5**: 789-800.
- Peckys, D. B. and N. de Jonge (2011). "Visualizing gold nanoparticle uptake in live cells with liquid scanning transmission electron microscopy." Nano Lett **11**(4): 1733-1738.
- Pogodin, S., J. Hasan, V. A. Baulin, H. K. Webb, V. K. Truong, T. H. Phong Nguyen, V. Boshkovikj, C. J. Fluke, G. S. Watson, J. A. Watson, R. J. Crawford and E. P. Ivanova (2013). "Biophysical model of bacterial cell interactions with nanopatterned cicada wing surfaces." Biophys J **104**(4): 835-840.
- Postek, M. T. and A. E. Vladár (2008). "Helium ion microscopy and its application to nanotechnology and nanometrology." Scanning **30**(6): 457-462.
- Proft, T. and E. N. Baker (2009). "Pili in Gram-negative and Gram-positive bacteria - structure, assembly and their role in disease." Cell Mol Life Sci **66**(4): 613-635.
- Reichert, W. and G. Truskey (1990). "Total internal reflection fluorescence (TIRF) microscopy. I. Modelling cell contact region fluorescence." Journal of cell science **96**(2): 219-230.
- Reith, F., S. Rogers, D. C. McPhail and D. Webb (2006). "Biomineralization of Gold: Biofilms on Bacterioform Gold." Science **313**: 233-236.
- Reynolds, T. B. and G. R. Fink (2001). "Bakers' Yeast, a Model for Fungal Biofilm Formation." Science **291**(5505): 878-881.
- Reynolds, T. B., A. Jansen, X. Peng and G. R. Fink (2008). "Mat formation in Saccharomyces cerevisiae requires nutrient and pH gradients." Eukaryot Cell **7**(1): 122-130.
- Richards, R. G., M. Stiffanic, G. R. Owen, M. Riehle, I. Ap Gwynn and A. S. Curtis (2001). "Immunogold labelling of fibroblast focal adhesion sites visualised in fixed material using scanning electron microscopy, and living, using internal reflection microscopy." Cell biology international **25**(12): 1237-1249.
- Ross, R. (1897). "On some Peculiar Pigmented Cells Found in Two Mosquitos Fed on Malarial Blood." British Medical Journal **2**(1929): 1786-1788.

- Roth, J. (1996). "The silver anniversary of gold: 25 years of the colloidal gold marker system for immunocytochemistry and histochemistry." Histochemistry and Cell Biology **106**(1): 1-8.
- Russell, S. D. and C. P. Daghlian (1985). "Scanning electron microscopic observations on deembedded biological tissue sections: Comparison of different fixatives and embedding materials." Journal of Electron Microscopy Technique **2**(5): 489-495.
- Rust, M. J., M. Bates and X. Zhuang (2006). "Sub-diffraction-limit imaging by stochastic optical reconstruction microscopy (STORM)." Nature methods **3**(10): 793.
- Ryan, O., R. S. Shapiro, C. F. Kurat, D. Mayhew, A. Baryshnikova, B. Chin, Z.-Y. Lin, M. J. Cox, F. Vizeacoumar, D. Cheung, S. Bahr, K. Tsui, F. Tebbji, A. Sellam, F. Istel, T. Schwarzmüller, T. B. Reynolds, K. Kuchler, D. K. Gifford, M. Whiteway, G. Giaever, C. Nislow, M. Costanzo, A.-C. Gingras, R. D. Mitra, B. Andrews, G. R. Fink, L. E. Cowen and C. Boone (2012). "Global Gene Deletion Analysis Exploring Yeast Filamentous Growth." Science **337**(6100): 1353-1356.
- Sarode, N., S. E. Davis, R. N. Tams and T. B. Reynolds (2014). "The Wsc1p cell wall signaling protein controls biofilm (Mat) formation independently of Flo11p in Saccharomyces cerevisiae." G3 (Bethesda) **4**(2): 199-207.
- Scherz, K., Andersen, R. Bojsen, L. Gro, Rejkjaer, Sorensen, M. Weiss, Nielsen, M. Lisby, A. Folkesson and B. Regenberg (2014). "Genetic basis for Saccharomyces cerevisiae biofilm in liquid medium." G3 (Bethesda) **4**(9): 1671-1680.
- Schindelin, J., I. Arganda-Carreras, E. Frise, V. Kaynig, M. Longair, T. Pietzsch, S. Preibisch, C. Rueden, S. Saalfeld, B. Schmid, J.-Y. Tinevez, D. J. White, V. Hartenstein, K. Eliceiri, P. Tomancak and A. Cardona (2012). "Fiji: an open-source platform for biological-image analysis." Nature Methods **9**: 676.
- Servetas, I., C. Berbegal, N. Camacho, A. Bekatorou, S. Ferrer, P. Nigam, C. Drouza and A. A. Koutinas (2013). "Saccharomyces cerevisiae and Oenococcus oeni immobilized in different layers of a cellulose/starch gel composite for simultaneous alcoholic and malolactic wine fermentations." Process Biochemistry **48**(9): 1279-1284.
- Siedentopf, H. and R. Zsigmondy (1902). "Uber sichtbarmachung und größenbestimmung ultramikoskopischer teilchen, mit besonderer anwendung auf goldrubingläser." Annalen der Physik **315**(1): 1-39.
- Simões, M., L. C. Simões and M. J. Vieira (2010). "A review of current and emergent biofilm control strategies." LWT - Food Science and Technology **43**(4): 573-583.
- Singer, C. (1914). "Notes on the early history of microscopy." Proceedings of the Royal Society of Medicine **7**(Sect_Hist_Med): 247-279.
- Smith, C. (2012). "Two microscopes are better than one." Nature **492**: 293.
- Sundstrom Paula (2002). "Adhesion in Candida spp." Cellular Microbiology **4**(8): 461-469.

- Sung-Hoon, H., H. Jaeyeon and L. Heon (2009). "Replication of cicada wing's nano-patterns by hot embossing and UV nanoimprinting." Nanotechnology **20**(38): 385303.
- Suzuki, E. (2002). "High-resolution scanning electron microscopy of immunogold-labelled cells by the use of thin plasma coating of osmium." Journal of Microscopy **208**(3): 153-157.
- Teparić, R., I. Stuparević and V. Mrša (2004). "Increased mortality of Saccharomyces cerevisiae cell wall protein mutants." Microbiology **150**(10): 3145-3150.
- Thodey, K., S. Galanie and C. D. Smolke (2014). "A microbial biomanufacturing platform for natural and semisynthetic opioids." Nat Chem Biol **10**(10): 837-844.
- Tofalo, R., G. Perpetuini, P. Di Gianvito, M. Schirone, A. Corsetti and G. Suzzi (2014). "Genetic diversity of FLO1 and FLO5 genes in wine flocculent Saccharomyces cerevisiae strains." Int J Food Microbiol **191c**: 45-52.
- Trejdosiewicz, L. K., M. A. Smolira, G. M. Hodges, S. L. Goodman and D. C. Livingston (1981). "Cell surface distribution of fibronectin in cultures of fibroblasts and bladder derived epithelium: SEM-immunogold localization compared to immunoperoxidase and immunofluorescence." Journal of Microscopy **123**(2): 227-236.
- Tsien, R. Y. (1998). "The Green Fluorescent Protein." Annual Review of Biochemistry **67**(1): 509-544.
- Verstrepen, K. J. and F. M. Klis (2006). "Flocculation, adhesion and biofilm formation in yeasts." Mol Microbiol **60**(1): 5-15.
- Watanabe, S., A. Punge, G. Hollopeter, K. I. Willig, R. J. Hobson, M. W. Davis, S. W. Hell and E. M. Jorgensen (2011). "Protein localization in electron micrographs using fluorescence nanoscopy." Nat Methods **8**(1): 80-84.
- Weaver, J. C., G. W. Milliron, A. Miserez, K. Evans-Lutterodt, S. Herrera, I. Gallana, W. J. Mershon, B. Swanson, P. Zavattieri, E. DiMasi and D. Kisailus (2012). "The Stomatopod Dactyl Club: A Formidable Damage-Tolerant Biological Hammer." Science **336**(6086): 1275.
- Wegst, U. G., H. Bai, E. Saiz, A. P. Tomsia and R. O. Ritchie (2015). "Bioinspired structural materials." Nat Mater **14**(1): 23-36.
- Wen, L., Y. Tian and L. Jiang (2015). "Bioinspired super-wettability from fundamental research to practical applications." Angew Chem Int Ed Engl **54**(11): 3387-3399.
- Wenzel, R. N. (1949). "Surface Roughness and Contact Angle." The Journal of Physical and Colloid Chemistry **53**(9): 1466-1467.
- Winzeler, E. A., D. D. Shoemaker, A. Astromoff, H. Liang, K. Anderson, B. Andre, R. Bangham, R. Benito, J. D. Boeke, H. Bussey, A. M. Chu, C. Connelly, K. Davis, F. Dietrich, S. W. Dow, M. El Bakkoury, F. Foury, S. H. Friend, E. Gentalen, G. Giaever, J. H. Hegemann, T. Jones, M. Laub, H. Liao, N. Liebundguth, D. J. Lockhart, A. Lucau-Danila, M. Lussier, N. M'Rabet, P. Menard, M. Mittmann, C. Pai, C. Rebischung, J. L. Revuelta, L. Riles, C. J. Roberts, P. Ross-MacDonald, B. Scherens, M. Snyder, S. Sookhai-Mahadeo, R. K. Storms, S. Véronneau, M. Voet, G. Volckaert, T. R. Ward, R.

Wysocki, G. S. Yen, K. Yu, K. Zimmermann, P. Philippsen, M. Johnston and R. W. Davis (1999). "Functional Characterization of the S. cerevisiae Genome by Gene Deletion and Parallel Analysis." Science **285**(5429): 901-906.
- Wisse, E. (2010). "Fixation methods for electron microscopy of human and other liver." World Journal of Gastroenterology **16**(23): 2851.
- Xu, L. C. and C. A. Siedlecki (2007). "Effects of surface wettability and contact time on protein adhesion to biomaterial surfaces." Biomaterials **28**(22): 3273-3283.
- Yang, J., D. C. Ferranti, L. A. Stern, C. A. Sanford, J. Huang, Z. Ren, L. C. Qin and A. R. Hall (2011). "Rapid and precise scanning helium ion microscope milling of solid-state nanopores for biomolecule detection." Nanotechnology **22**(28): 285310.
- Zhang, S., J. Huang, Y. Cheng, H. Yang, Z. Chen and Y. Lai (2017). "Bioinspired Surfaces with Superwettability for Anti-Icing and Ice-Phobic Application: Concept, Mechanism, and Design." Small **13**(48): 1701867-n/a.
- Zhang, X. and Z. Liu (2008). "Superlenses to overcome the diffraction limit." Nature materials **7**(6): 435.
- Zheng, Y., H. Bai, Z. Huang, X. Tian, F. Q. Nie, Y. Zhao, J. Zhai and L. Jiang (2010). "Directional water collection on wetted spider silk." Nature **463**(7281): 640-643.
- Zsigmondy, R. (1926). Properties of colloids. Nobel Lecture.

APPENDIX A

POSTER

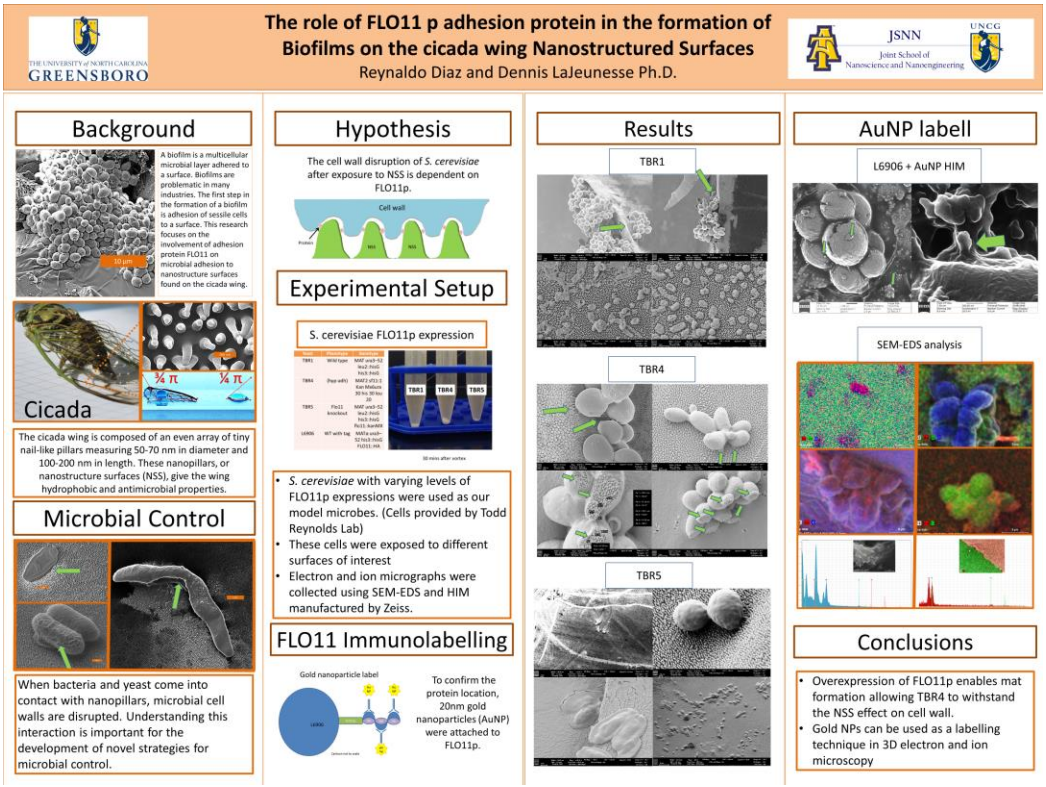

S. Image: 1 Poster Summarizing the work of this document.

APPENDIX B

LIST OF ABBREVIATIONS

1. CLM-Confocal Laser Microscope
2. AFM- Atomic Force Microscopy
3. SPBM-Scanning particle beam Microscopy
4. TEM-Transmission Electron Microscopy
5. EM-Electron Microscopes
6. STEM-Scanning transmission electron microscopy
7. SEM-Scanning Electron Microscope
8. HIM-Helium Ion Microscope
9. EDS- Energy Dispersive X-ray Spectrometry
10. BSE-Backscattered Electrons
11. SEM-EDS- scanning electron microscope equipped with energy dispersive spectrometry
12. AuNP-Gold Nanoparticle
13. CW-Cicada Wing
14. NSS-Nano Structured Surfaces
15. TIRF-total internal reflection fluorescence
16. PALM-photoactivated localization microscopy
17. STORM-stochastic optical reconstruction microscopy)
18. FOV-field of view (p.32)
19. SE-Secondary electrons (p.33)
20. HA-human influenza hemagglutinin epitope tag